

# UC Davis

## UC Davis Previously Published Works

### Title

Sarcoplipin Exhibits Abundant RNA Transcription and Minimal Protein Expression in Horse Gluteal Muscle

### Permalink

<https://escholarship.org/uc/item/50s9x7qt>

### Journal

Veterinary Sciences, 7(4)

### ISSN

2306-7381

### Authors

Autry, Joseph M  
Karim, Christine B  
Perumbakkam, Sudeep  
[et al.](#)

### Publication Date

2020

### DOI

10.3390/vetsci7040178





### Copyright Information

This work is made available under the terms of a Creative Commons Attribution License, available at <https://creativecommons.org/licenses/by/4.0/>

Peer reviewed

Article

# Sarcoplipin Exhibits Abundant RNA Transcription and Minimal Protein Expression in Horse Gluteal Muscle

Joseph M. Autry <sup>1,\*</sup>, Christine B. Karim <sup>1</sup>, Sudeep Perumbakkam <sup>2</sup>, Carrie J. Finno <sup>3</sup>,  
Erica C. McKenzie <sup>4</sup>, David D. Thomas <sup>1,†</sup> and Stephanie J. Valberg <sup>2,\*</sup>

<sup>1</sup> Department of Biochemistry, Molecular Biology, and Biophysics, University of Minnesota, Minneapolis, MN 55455, USA; christine.karim@gmail.com (C.B.K.); ddt@umn.edu (D.D.T.)

<sup>2</sup> Department of Large Animal Clinical Sciences, McPhail Equine Performance Center, Michigan State University, East Lansing, MI 48823, USA; perumbakkam@gmail.com

<sup>3</sup> Department of Population Health and Reproduction, University of California, Davis, CA 95616, USA; cjfinno@ucdavis.edu

<sup>4</sup> Department of Clinical Sciences, Oregon State University, Corvallis, OR 97331, USA; erica.mckenzie@oregonstate.edu

\* Correspondence: jma@ddt.umn.edu (J.M.A.); valbergs@msu.edu (S.J.V.)

† Co-Senior Authors: ddt@umn.edu (D.D.T.) and valbergs@msu.edu (S.J.V.)

Received: 22 October 2020; Accepted: 5 November 2020; Published: 13 November 2020



**Abstract:** Ca<sup>2+</sup> regulation in equine muscle is important for horse performance, yet little is known about this species-specific regulation. We reported recently that horse encode unique gene and protein sequences for the sarcoplasmic reticulum (SR) Ca<sup>2+</sup>-transporting ATPase (SERCA) and the regulatory subunit sarcoplipin (SLN). Here we quantified gene transcription and protein expression of SERCA and its inhibitory peptides in horse gluteus, as compared to commonly-studied rabbit skeletal muscle. RNA sequencing and protein immunoblotting determined that horse gluteus expresses the *ATP2A1* gene (SERCA1) as the predominant SR Ca<sup>2+</sup>-ATPase isoform and the *SLN* gene as the most-abundant SERCA inhibitory peptide, as also found in rabbit skeletal muscle. Equine muscle expresses an insignificant level of phospholamban (PLN), another key SERCA inhibitory peptide expressed commonly in a variety of mammalian striated muscles. Surprisingly in horse, the RNA transcript ratio of *SLN*-to-*ATP2A1* is an order of magnitude *higher* than in rabbit, while the corresponding protein expression ratio is an order of magnitude *lower* than in rabbit. Thus, *SLN* is not efficiently translated or maintained as a stable protein in horse muscle, suggesting a non-coding role for supra-abundant *SLN* mRNA. We propose that the lack of *SLN* and *PLN* inhibition of SERCA activity in equine muscle is an evolutionary adaptation that potentiates Ca<sup>2+</sup> cycling and muscle contractility in a prey species domestically selected for speed.

**Keywords:** equidae; gene expression profiling; intracellular membranes; long noncoding RNA; peptides; rhabdomyolysis; sarcoplipin; protein subunits; sarcoplasmic reticulum calcium-transporting ATPases; western blotting

## 1. Introduction

SERCA is a prototypical member of the P-type ion-motive transport ATPase family: central to active membrane transport [1,2]. SERCA Ca<sup>2+</sup>-transporting ATPases are encoded by a family of three genes (*ATP2A1*, *ATP2A2*, and *ATP2A3*) that produce protein isoforms SERCA1 (expressed typically in fast-twitch myofibers), SERCA2 (slow-twitch myofibers, cardiomyocytes, and non-muscle cells), and SERCA3 (smooth muscle cells, platelet cells, and non-muscle cells), respectively. The Ca<sup>2+</sup> transport activity of SERCA is regulated by a family of single-pass transmembrane peptides in SR,

including sarcolipin (SLN) and phospholamban (PLN). SLN and PLN were discovered in the early 1970s [3,4] and have since been characterized as potent regulators of contractility, dependent upon post-translational modifications and protein expression level [5–9]. Recently, five additional peptide regulators of SERCA have been reported in mouse: the inhibitor myoregulin (MRLN) in muscle, the inhibitor small ankyrin 1 (sAnk1) in muscle, the activator dwarf open reading frame (DWORF) in ventricles, the inhibitor endoregulin (ELN) in endothelial and epithelial cells, and the inhibitor “another-regulin” (ALN) in non-muscle tissues [10–14].

The roles of SERCA regulatory peptides in horse SR function are unknown. In mammals such as rabbit, dog, and pig, SLN is the primary regulatory peptide expressed in fast-twitch skeletal muscle [7,15–17]. SLN inhibits SERCA activity through multiple enzymatic mechanisms by decreasing maximal velocity ( $V_{max}$ ), by decreasing  $Ca^{2+}$  binding affinity ( $1/K_{Ca}$ ), and by decreasing the number of  $Ca^{2+}$  ions transported per ATP molecule hydrolyzed (coupling stoichiometry) below the optimal  $Ca^{2+}$ /ATP coupling ratio of two [18–26]. SLN inhibition is relieved in part by phosphorylation and de-acylation [6,27,28], resulting in enhanced SR  $Ca^{2+}$  uptake. To optimize myoplasmic  $Ca^{2+}$  cycling for muscle performance, SERCA uptake activity must be fine-tuned in balance with  $Ca^{2+}$  release activity via the SR  $Ca^{2+}$  channel Ryanodine Receptor (RZR). The skeletal muscle isoform RZR1 is regulated by myoplasmic and luminal  $Ca^{2+}$  levels, plus  $Ca^{2+}$ -regulated proteins such as calsequestrin, calmodulin-dependent protein kinase, and calmodulin [29–31].

Valberg et al. reported recently the deduced protein sequence and the gene expression level of *SLN*, *MRLN*, and *DWORF* in skeletal muscle of three horse breeds: Thoroughbred, Standardbred, and Quarter Horse [32]. As in other large mammals, the *SLN* gene in horse gluteus is the highest expressed RNA transcript in the family of SERCA regulatory peptides [32]. Phylogenomic analyses of SLN protein sequences across 131 vertebrate species [33] demonstrated that horse SLN has novel deletions and replacements of residues that are predicted to control SERCA regulation and function [7,18,26,32,34]. The horse *SLN* gene encodes a 29-residue peptide [32], in contrast with a consensus 31-residue length for orthologous SLN peptides encoded by 100+ species from five vertebrate classes: mammal, bird, reptile, amphibian, and fish [7,26,32,33]. Uniquely, horse SLN is the only reported ortholog [32,33] missing all four regulatory sites that are common in other species: Ser4 and Thr5 for SLN phosphorylation and relief of SERCA inhibition [6,27]; Cys9 for SLN acylation and relief of SERCA uncoupling [7,28]; and Tyr31 for SERCA interaction, organelle targeting of SLN, and potential luminal nitration of SLN [34–38]; as assessed using residues numbered via the consensus 31-amino acid length, e.g., encoded by rabbit, mouse, and human *SLN* genes [32]. The unique amino acid sequence of horse SLN was also identified in additional *Equus* species such as Zebra and Przewalski horse but not in other species from the perissodactyl order, such as the *Rhinocerotidae* and *Tapiridae* families [32,33]. Thus horses, with natural selection as prey animals and subsequent selective breeding for performance, may have developed highly adapted mechanisms for  $Ca^{2+}$  transport regulation including control of SERCA activity by SLN.

Horses are susceptible to exertional rhabdomyolysis, with a 3% incidence reported across breeds, including a 4% incidence in endurance Arabians and a 7–10% incidence specific to racehorses [39–41]. The molecular mechanism that causes the high susceptibility of horse to rhabdomyolysis is unknown; however, a common pathway for rhabdomyolysis seems to be associated with aberrant SR  $Ca^{2+}$  regulation [42]. Dantrolene, which inhibits  $Ca^{2+}$  release through RZR1 in SR, is a muscle relaxant that is used often to treat rhabdomyolysis in horses [43–45], thereby supporting further the  $Ca^{2+}$ -linkage hypothesis. We propose that further investigation of  $Ca^{2+}$  cycling in horse muscle will provide insights into unique adaptations for athletic prowess, plus identify molecular targets for potential treatment of rhabdomyolysis in horse breeds.

The goal of this study was to compare gene and protein expression of SERCA, SLN, and PLN in healthy horse muscle, with comparison to the commonly studied model of rabbit skeletal muscle. Our research identified unique steady-state levels of RNA transcription and protein expression for SLN, and these findings were interpreted in light of the high susceptibility of horses to exertional

rhabdomyolysis. We propose that SERCA activity and SLN regulation in horse SR differs from the SERCA-SLN system in rabbit SR, based on unique sequences and expression levels of horse orthologs. We hypothesize that comparative studies of gene expression and biochemical regulation of SR enzymes will increase the broader understanding of selective adaptation of horse and human muscle, with a specific focus towards performance and disease.

## 2. Materials and Methods

### 2.1. Sequences

The Enzyme Commission number (EC) for the SERCA Ca<sup>2+</sup>-transporting ATPase is EC 7.2.2.10 in the IUBMB Enzyme Database. The enzyme for an EC number can be identified through the ExplorEnz utility [46].

The GenBank accession code for cDNA sequences of target proteins and respective species orthologs are as follows: (1) SERCA1a: horse XM\_001502262.6, rabbit ABW96358.1, mouse BC036292.1 [47], and human NM\_004320.4 [48]. (2) SLN: horse [32], rabbit U96091.1 [49], mouse NM\_025540.2, and human U96094.1 [49]. (3) PLN: horse [32], rabbit Y00761.1 [50], human M63603.1 [51], and dog NM\_001003332.1 [52]. (4) MRLN: horse [32] and human NM\_001304732.2 [10]. (5) DWORF: horse [32] and mouse NM\_001369305.1 [12]. (6) GP: horse muscle NP\_001138725.1, rabbit muscle NP\_001075653.1, and human muscle AH002957.2. The cDNA sequence for an accession code can be identified through the NCBI GenBank utility [53].

### 2.2. Animals and Samples

Six healthy endurance Arabian horses (13.0 ± 6.2 yr, with four castrated males and two females) were used for transcriptomic analyses. Percutaneous needle biopsies had previously been obtained from a standardized site on the gluteus medius muscle [54]. Owner consent was obtained with IACUC approval from Oregon State University with ACUP # 4480.

Protein immunoblotting required 200 g of muscle in order to isolate highly-purified SR membranes [55–58]. This necessitated euthanasia, and therefore horses donated to the University of Minnesota due to severe orthopedic lameness, were used for biochemical studies of muscle SR proteins [58]. Muscle samples were obtained from four horses aged 10–18 years: three castrated males (two Quarter Horses and one Thoroughbred) and one female (Quarter Horse). Horse owners provided written consent for obtaining samples for this research, with IACUC protocol # 1511-33199A.

For SR isolation from rabbit skeletal muscle, New Zealand white rabbits (junior does less than six months of age) were provided by the Research Animal Resources Facility at the University of Minnesota. Euthanasia of rabbits was performed with appropriate palliative care consistent with American Veterinary Medical Association guideline, with IACUC protocol # 1611-34327A [58].

### 2.3. Muscle Fiber Type Composition

Muscle fiber type composition was determined using a myosin ATPase assay of sections obtained from gluteal muscle that had been frozen in liquid nitrogen-chilled isopentane as previously described [59]. For comparison to horse gluteal muscle, the muscle fiber type composition of seven back and leg muscles from 3–12 rabbits were compiled from the report by Leberer and Pette [60].

### 2.4. RNA Sequencing of the Horse Muscle Transcriptome

RNA-seq generation of these samples was described previously [59]. In brief, frozen gluteal muscle was ground to powder, and total RNA was extracted. Quantification and quality of RNA were assessed. Samples with an RNA integrity number (RIN) ≥ 7 were used for library preparation and quantification. The library was constructed using a strand-specific polyA<sup>+</sup> capture protocol (TruSeq Stranded mRNA Kit, Illumina, Inc.). Sequencing was performed using the Illumina HiSeq 2000 genome analyzer (100 base-pair paired-ends) at a targeted 35 million reads/sample. A total of

26,993 transcript sequences from the Ensembl EquCab 2.86 database [61] were used to create the index file and map RNA-seq reads. Samples that passed the quality threshold ( $Q \geq 30$ ) were aligned to the horse transcriptome index using Salmon program 0.11.0 [62]. Count data, generated as transcripts per million reads (TPM) by Salmon processing, were used to compile gene expression for each individual sample ( $N \geq 5$  horses per transcript). The RNA-seq datasets [59] are available in the NCBI Gene Expression Omnibus [63] with GEO accession number GSE104388 [59] and deposited in the Sequence Read Archive (SRA) database with accession number SRP082284.

### 2.5. RNA-seq Quantitation of Gene Expression in Horse and Rabbit Muscle

RNA-seq analyses were performed as previously described [59]. Gene expression of seven targets (*ATP2A1*, *ATP2A2*, *ATP2A3*, *SLN*, *PLN*, *DWORF*, and *MRLN*) was extracted from RNA-seq data, normalized based on the length of each transcript and the overall sequencing depth per individual horse, and expressed as transcripts per million (TPM). The values for mean, range, and standard deviation of gene expression are reported as TPM (Figure 1). For comparison, RNA-seq data of gene expression in rabbit muscle (*ATP2A1*, *ATP2A2*, *SLN*, and *MRLN*) were mined from SRA accession number SAMN00013649<sup>3</sup> (rabbit species *Oryctolagus cuniculus*) (Figure 1).

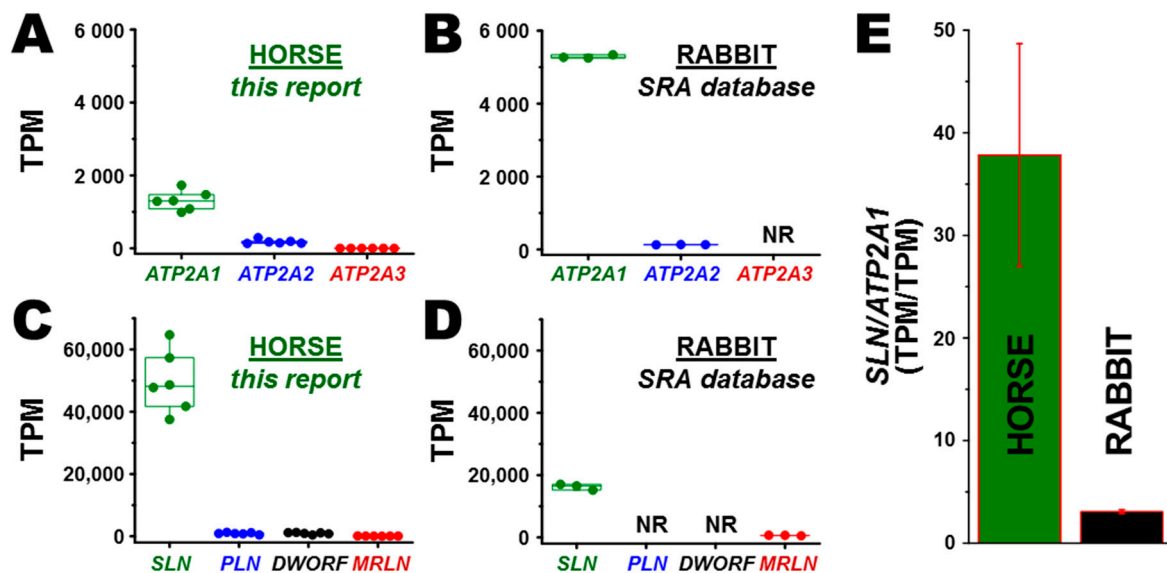


**Figure 1.** RNA-seq quantitation of gene transcription for calcium regulatory proteins in horse muscle. (A–D) The number of target transcripts per million reads (TPM) are reported, using a box plot to indicate the median, maximum, minimum, and range ( $N = 6$  Arabian horses and  $N = 3$  rabbits). (A,B) *ATP2A1* (*SERCA1*), *ATP2A2* (*SERCA2*), and *ATP2A3* (*SERCA3*) in horse gluteus and rabbit muscle, respectively. (C,D) *SLN*, *PLN*, *DWORF*, and *MRLN* in horse gluteus and rabbit muscle, respectively. (E) The relative ratio of transcript/transcript expression (TPM/TPM) of *SLN* to *ATP2A1* in horse gluteus and rabbit muscle, respectively. The expression level of horse genes was mined from RNA-seq data with SRA accession number SRP082284. The expression level of rabbit genes were mined from RNA-seq data reported with SRA accession number SAMN00013649. (D) NR indicates “data not reported” for rabbit gene transcripts in the SRA database.

### 2.6. Purification of SR Vesicles from Horse Gluteal Muscle

Following humane euthanasia of donated horses, one middle gluteal muscle per horse was harvested, and mechanical disruption and differential centrifugation were used to isolate SR vesicles [58]. Horse SR vesicles are defined as the centrifugal pellet isolated at  $10,000 \times g_{max}$  for 20 min (the “10KP” cellular fraction), which was preceded by two clarification spins at  $4000 \times g_{max}$  for 20 min (see our horse

SR protocol flow-chart reported as Figure 1 in [58]). The protein concentration of horse SR vesicles was determined by the BCA assay (Pierce Biotechnology).

### 2.7. Purification of SR Vesicles from Rabbit Skeletal Muscle

Following humane euthanasia of rabbits, the back and leg muscles per rabbit were harvested, and mechanical disruption and differential centrifugation were used to isolate SR vesicles [58,64]. Rabbit SR vesicles are defined as the centrifugal pellet isolated at  $23,000\times g_{max}$  for 60 min (the “23KP” cellular fraction), which was preceded by three clarification spins:  $4000\times g_{max}$  for 20 min,  $4000\times g_{max}$  for 20 min, and  $12,000\times g_{max}$  for 20 min (see the rabbit SR protocol flow-chart reported as Figure S1 in [58]). The protein concentration of rabbit SR vesicles was determined by the BCA assay (Pierce Biotechnology).

### 2.8. Synthesis of SLN Peptide Orthologs for Quantitative Immunoblotting

Horse SLN (29 residues), rabbit SLN (31 residues), and human SLN (31 residues) peptides were synthesized by New England Peptides, Inc., using Fmoc solid-phase chemistry at 50-mg crude scale (16  $\mu$ mol). Quality assessment of peptide synthesis was validated using high-performance liquid chromatography (HPLC) and mass spectrometry. The three SLN peptides were synthesized with an acetylated N-terminus and an amidated C-terminus. Synthetic SLN peptides were further purified in-house by HPLC [65]. The concentration of synthetic SLN peptides was determined by amino acid analysis, BCA assay, and densitometry of Coomassie blue-stained gels [34,66]. Laemmli-type SDS-PAGE gels were purchased from Bio-Rad Laboratories, Inc.

### 2.9. Quantitative Immunoblotting of Muscle Proteins

Immunoblotting was performed as previously described [55,56,67,68]. Proteins separated by SDS-PAGE were transferred to a PVDF membrane (0.2- $\mu$ m pore Immobilon-FL) using a solution of 25 mM Tris, 192 mM glycine, pH 8.3. PVDF blots were blocked using Odyssey-TBS blocking buffer (LI-COR Biosciences, Inc., Lincoln, NE, USA). Primary antibodies are described below. Primary antibodies were used typically at 1:1000 dilution, with incubation for 16–18 h at 4 °C. Secondary antibodies (fluorescently-labeled) were used at 1:15,000 dilution, with incubation for 20 min at 4 °C. After incubation with primary or secondary antibody, blots were washed three times with Tris-buffered saline (pH 7.4) with 0.05% Tween-20, and then once with Tris-buffered saline (pH 7.4) without Tween-20. Sandwich-immunolabeling of the target protein via primary plus secondary antibodies was detected using an LI-COR laser scanner in near-infrared fluorescence mode equipped with Odyssey acquisition software, and bands were quantified using Image Studio Lite software (LI-COR Biosciences, Inc.) on a local PC computer (see next section).

### 2.10. Secondary Immunolabeling and Target Quantitation Using Fluorescent Anti-IgG Antibodies

Secondary antibodies labeled with near-infrared fluorophore (700 nm or 800 nm emission) were purchased from LI-COR Biosciences, including affinity-purified goat antisera against mouse IgG (goat anti-mouse pAb) and affinity-purified goat antisera against rabbit IgG (goat anti-rabbit pAb). Secondary antibodies were used at 1:15,000 dilution (20 min at 4 °C) for sandwich-labeling of target protein following primary antibody incubation. Fluorescent bands were detected using an Odyssey laser scanner in near-infrared mode and quantified using Image Studio Lite software (LI-COR Biosciences, Inc.). For quantitative comparison of band intensities via Image Studio Lite, a box was drawn around the band of interest, and the fluorescence intensity was extracted using LI-COR software. For each immunoblot, the background intensity was determined by drawing a same-sized box (as target band) in a protein-free lane, and this background intensity was subtracted from the target protein signal. For a target protein that showed multiple oligomeric species, the intensity of each monomeric and oligomeric band was quantitated and then added together for a sum total of target per sample. For quantitative standard, a synthetic peptide of SLN or PLN were utilized as appropriate, with the peptide



standard loaded in multiple amounts (low nanogram range), followed by linear-regression analysis of immunoblot intensity versus protein load [55–57,68].

### 2.11. Custom Anti-Horse-SLN Polyclonal Antibody GS3379

Due to sequence divergence of horse SLN at the N-and C-termini compared to rabbit, mouse, and human orthologs, we designed and purchased an anti-horse-SLN polyclonal antibody from Genscript (pAb GS3379). The immunogen was a 6-residue N-terminal peptide of horse SLN (Q<sup>1</sup>MEWRRE<sup>6</sup>C), with an added <sup>-1</sup>Gln residue (to mimic an acetylated N-terminus) along with an added <sup>+7</sup>Cys residue (to serve as a C-terminal linker). The horse N-terminal SLN peptide was conjugated to keyhole limpet hemocyanin (KLH) as the carrier protein for rabbit immunization. The anti-horse-SLN pAb GS3379 was purified from rabbit serum using affinity purification on the same horse-SLN-peptide coupled as an affinity-column ligand. Antibody generation, affinity purification, and titer determination were performed by Genscript. Here pAb GS3379 was used for primary labeling at 1:1000 dilution (0.4 µg/mL). pAb GS3379 was validated using synthetic horse SLN as a quantitative immunoblot standard (Figure 2). It is readily apparent that SR vesicles from horse gluteal muscle express a minimal amount of SLN (Figures 2 and 3, Figure S2), at sub-stoichiometric amounts compared to SERCA. The low expression of SLN in horse gluteal muscle SR was previously demonstrated in preliminary immunoblot experiments during the development of the isolation procedure for horse SR vesicles [69], as utilized in this publication.

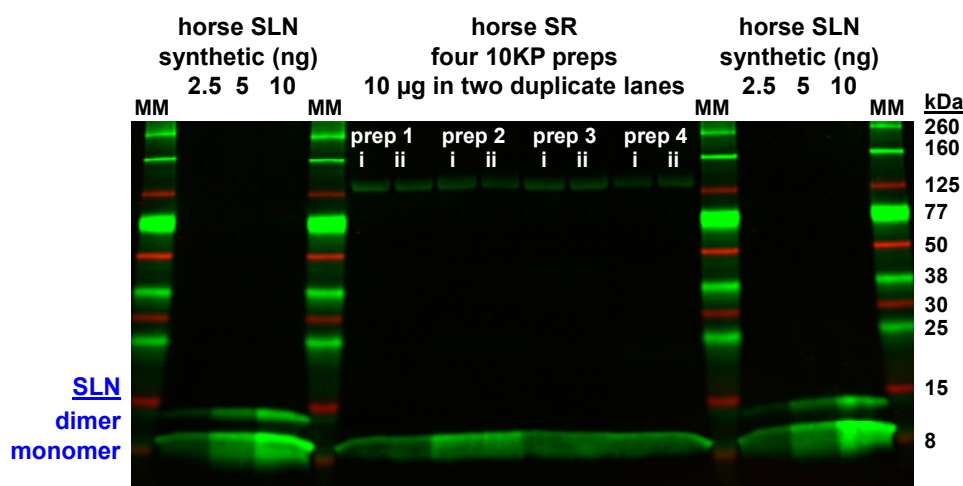


**Figure 2.** Immunoblot analysis using custom anti-horse-SLN pAb GS3379 detects minimal expression of SLN protein in horse SR vesicles. The primary antibody was the custom anti-horse-SLN pAb GS3379, with immunogen comprising horse residues <sup>1</sup>MEWRRE<sup>6</sup>. Samples were electrophoresed through a 4–20% Laemmli gel. Horse SR vesicles were assayed (N = 4 preps; 10 µg protein per lane; each prep run in duplicate lanes). Synthetic horse SLN was used as a quantitative standard (2.5, 5, or 10 ng/lane) in duplicate sets on left and right sides on the gel. Immunoblotting was performed using pAb GS3379 (primary) and goat anti-rabbit-IgG pAb labeled with 800-nm fluorophore (secondary). Immunolabeling was quantified using the LI-COR laser scanner system. Protein gel markers (kDa) are indicated on the right. Two putative molecular species of SLN on SDS-PAGE (monomer and dimer) are indicated by blue text on the left.

### 2.12. Custom C-Terminal Anti-Rabbit/Mouse/Human-SLN Polyclonal Antibody PFD-1

Dr. Patrick F. Desmond and Professor Robert J. Bloch, from the University of Maryland School of Medicine, provided a custom-generated anti-SLN pAb [70]. Two immunogens were used for rabbit immunization: a base 7-residue C-terminal peptide conserved in rabbit/mouse/human SLN with alternate variations in SLN immunogenic peptides at N-and C-termini positions (acetyl-<sup>25</sup>LVRSYQY<sup>31</sup>-amide and C-amino hexanoic acid-<sup>25</sup>LVRSYQY<sup>31</sup>-OH). Both SLN peptides were

individually conjugated to BSA. Antibody generation and affinity purification were performed by 21st Century Biochemicals, Inc. The anti-rabbit/mouse/human-SLN pAb PFD-1 was validated for immunoblotting using mouse skeletal muscle homogenate and recombinant mouse SLN [70]. Horse SLN encodes <sup>24</sup>LVRYSQ<sup>29</sup> (i.e., horse SLN is missing one residue of the seven-residue immunogen: the terminal Tyr residue comprising the pAb PFD-1 epitope). Here pAb PFD-1 was used for primary labeling at 1:1000 dilution. Although horse SLN encodes six of seven residues in the immunogen peptide sequence, horse SR vesicles show significantly lower labeling than rabbit SR vesicles by pAb PFD-1 (Figure S2).

### 2.13. Commercial Anti-SLN Polyclonal Antibodies

Two anti-SLN commercial antibodies were purchased. One commercial anti-SLN antibody (ABT13) was raised against the mostly conserved C-terminus of SLN. One commercial anti-SLN antibody (pAb 18395-1-AP) was raised against human SLN (N-terminal peptide or full-length protein). Immunoblot conditions and validation reports for commercial anti-SLN antibodies are described as follows:

(1) Anti-SLN ABT13 is an affinity-purified rabbit pAb (Millipore Sigma). The immunogen was C-terminal residues <sup>26</sup>VRSYQY<sup>31</sup> of rabbit/mouse/human SLN as a sulfolink-peptide (CGG-<sup>26</sup>VRSYQY<sup>31</sup>) conjugated to KLH. Horse SLN encodes <sup>26</sup>VRSYQ<sup>30</sup> (i.e., missing the terminal Y31 of the rabbit/mouse/human SLN immunogen). Millipore Sigma reports that ABT13 reacts with rabbit, mouse, and human SLN on immunoblot at 1.5 µg/mL pAb, as corroborated here for rabbit SLN using 0.5 µg/mL pAb ABT13 (1:1000 dilution) and fluorescent secondary antibody detection (Figure 3). pAb ABT13 has been validated for SLN immunoblotting using human right atrium homogenate [71] and mouse soleus and diaphragm homogenates [72]. Here pAb ABT13 was used for primary labeling at 1:1000 dilution, with positive detection of SLN in rabbit SR vesicle, plus sunthetic rabbit and human SLN (Figure 3).

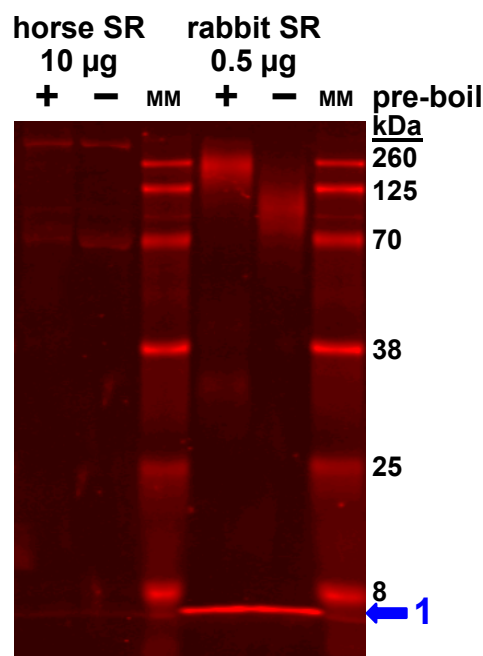


**Figure 3.** Immunoblot analysis using commercial anti-rabbit/mouse/human-SLN pAb ABT13 identifies SLN protein expression in rabbit SR vesicles, but not in horse SR. The primary antibody was the commercial anti-SLN pAb ABT13, with immunogen comprising rabbit/mouse/human SLN residues <sup>27</sup>RSYQY<sup>31</sup>, whereas horse SLN encodes <sup>26</sup>RSYQ<sup>29</sup>. Samples were electrophoresed through a 10% Laemmli gel. Horse SR vesicles were loaded at 10 µg protein per lane (left), and rabbit SR vesicles were loaded at 0.5 µg protein per lane (right). Immunoblotting was performed using pAb ABT13 (primary)



and goat anti-rabbit-IgG pAb labeled with 680-nm fluorophore (secondary). Immunolabeling was quantified using the LI-COR laser scanner system. Prior to electrophoresis, one sample of each SR prep was heated at 100 °C for 2 min in Laemmli sample buffer (+ pre-boil). Protein gel markers (kDa) are indicated on the right. The putative monomeric form of SLN on SDS-PAGE is indicated by the blue arrow with number 1 on the right.

(2) Anti-human-SLN 18395-1-AP is an affinity-purified rabbit pAb (Proteintech Group, Inc.). The immunogen was human SLN (residues 1–31) conjugated as a fusion protein to glutathione S-transferase (GST). Compared to human SLN protein, horse SLN is 77% identical (5 sequence variations and 2 deletions), and rabbit SLN is 81% identical (6 sequence variations) [32,33]. Proteintech Group reports that pAb 18395-1-AP reacts with SLN in human and mouse heart homogenates on immunoblot using antibody concentration of 1.6 µg/mL and 0.5 µg/mL pAb, respectively. pAb 18395-1-AP has been validated on SLN immunoblot using mouse heart homogenate [73]. Here pAb 18395-1-AP was used for primary labeling at 1:1000 dilution, a condition where pAb 18395-1-AP did not detect rabbit or horse SLN but instead showed (non-specific?) binding to other proteins in rabbit and horse SR (Figure S1).

#### 2.14. Anti-PLN Monoclonal Antibody 2D12

Anti-PLN antibody 2D12 is a mouse mAb (IgG2a isotype) generated by Dr. Larry R. Jones [74]. The immunogen of mAb 2D12 was residues 2–25 of dog PLN conjugated to thyroglobulin using glutaraldehyde. The epitope for mAb 2D12 is residues <sup>7</sup>LTRSAIR<sup>13</sup> of dog PLN [75], a sequence which is identical for horse and rabbit PLN [32]. mAb 2D12 (ab2685) was purchased from Abcam, P.L.C., as a stock solution of Ascites fluid diluted to 1 mg/mL mAb protein in PBS. Abcam reports that mAb 2D12 reacts on immunoblot with PLN peptides expressed in rabbit, mouse, human, pig, sheep, chicken, guinea pig, and dog tissues. mAb 2D12 has been validated for quantitative immunoblotting using multiple types of PLN samples: native and recombinant dog PLN, native mouse PLN, native human PLN, synthetic human PLN, and synthetic pig PLN [55–57,67,68,74,76,77]. Here anti-PLN mAb 2D12 was used for primary labeling at 1:1000 dilution (1 µg/mL), with successful detection of synthetic human PLN and horse PLN, as utilized as standards for quantitative immunoblotting (Figure 4). It is readily apparent that SR vesicles from horse gluteal muscle express an insignificant level of PLN.

#### 2.15. Experimental Design, Statistical Analysis, and Data Presentation

Biochemical assays were performed using independent SR vesicle preparations from N = 4 horses. Data analyses were performed using Microsoft Excel. Data graphs were generated using OriginLab 9.2 (Northampton, MA, USA). Scientists were not blinded to sample identity during data acquisition or analysis. Western blot analysis, i.e., signal intensity, was quantified using the LI-COR laser scanner system, via the associated Odyssey acquisition and Image Studio Lite analysis programs, provided by LI-COR, Inc. Data acquired in this study are presented in mean ± standard deviation.

### 3. Results

#### 3.1. Muscle Fiber Type Composition

The middle gluteal muscle of six healthy Arabian horses had a composition of type 1 myofibers with 17 ± 2% (slow-twitch), plus type 2A myofibers with 52 ± 8% (fast-twitch glucoxidative) and type 2X (fast-twitch) with 31 ± 8%, thereby expressing a 4.9 ± 0.9 fold greater abundance of fast-twitch myofibers [59]. For comparison, a compilation of seven types of rabbit white back and leg muscles shows a predominance of fast-twitch myocytes (type 2A with 21 ± 7.6% and type 2B with 76 ± 8.7%) versus slow-twitch myocytes (type I = 3.1 ± 3.1%) [60]. Although horse gluteal muscle has a greater percentage of type 1 slow-twitch myofibers than rabbit skeletal muscle ( $p < 0.0001$ ), the predominance

of fast-twitch myofibers in horse gluteus and rabbit muscle allows suitable comparison of SERCA1 and its control by peptide regulators.

### 3.2. Transcription of ATP2A Genes Encoding SERCA Proteins

Transcriptomic analysis identified the *ATP2A1* gene encoding SERCA1 as the predominant SERCA isoform expressed in the middle gluteal muscle of horse at  $7.3 \pm 2.8$  fold greater level than the *ATP2A2* gene encoding SERCA2 (Figure 1A). The middle gluteal muscle of horse showed insignificant expression of the horse *ATP2A3* gene, which is transcribed at a level comprising  $\sim 0.04\%$  of total transcripts from the *ATP2A* gene family (TPM/TPM) (Figure 1A). In rabbit, mined RNA-seq data demonstrated that the *ATP2A1* gene (SERCA1) is expressed at  $41 \pm 1.0$  fold greater level than the *ATP2A2* gene (SERCA2) (Figure 1B). Thus, both horse gluteal muscle and rabbit skeletal muscle express predominantly the *ATP2A1* gene, thereby providing a valid platform for comparative transcriptomic and biochemical analyses of SR function in these predominantly fast-twitch muscles.

### 3.3. Transcription of SERCA Regulatory Peptide Genes: *SLN*, *PLN*, *MRLN*, and *DWOLF*

*SLN* is the predominant regulatory peptide transcribed in horse gluteal muscle, with  $>55$ -fold greater expression than *PLN* and *DWOLF* and  $780 \pm 420$  fold greater expression than *MRLN* (Figure 1C). Transcription of the *SLN* gene is  $38 \pm 11$ -fold greater than *ATP2A1* (SERCA1), thereby demonstrating that the *SLN* gene is highly expressed in the horse gluteus muscle (Figure 1A,C,E).

A compilation of reported data (SRA database) from three laboratory rabbits indicated that the *SLN* gene is the predominant regulatory peptide transcribed in rabbit skeletal muscle, with  $26 \pm 4.3$ -fold greater gene expression than *MRLN* (Figure 1D). When comparing the relative ratio of gene expression of *SLN* to the sum of *ATP2A* genes, rabbit muscle shows a transcription ratio of  $3.1 \pm 0.19$  for *SLN*-to-*ATP2A1* (TPM/TPM), a ratio which is  $\sim 12$ -fold lower than the *SLN*-to-*ATP2A1* ratio in horse muscle (Figure 1B,D,E). Thus, our RNA-seq data is consistent with previous qRT-PCR studies indicating that *SLN* RNA is the predominant regulatory gene transcribed in fast-twitch muscle of the horse, similar to other non-rodent mammals such as rabbit and pig [15,32]. *MRLN* is reported to be the primary regulatory peptide gene expressed in mouse skeletal muscle [10].

### 3.4. Expression of the *SLN* Peptide Relative to SERCA Protein in Horse SR vesicles, as Detected by Multiple Anti-*SLN* Antibodies

To determine if *SLN* peptide expression correlates with *SLN* gene transcription, immunoblotting was used to quantitate the expression level of native *SLN* peptide in horse muscle (Figures 2 and 3, Figures S1 and S2). Due to the unique amino acid sequence of horse *SLN* [32], a custom anti-horse-*SLN* pAb was ordered (GS3379) using horse *SLN* residues <sup>1</sup>MEWRRE<sup>6</sup> (N-terminal peptide) as immunogen. In addition, a full-length equine *SLN* peptide (amino acids 1–29) was synthesized as a positive control for quantitative immunoblotting [55,56]. On immunoblots, anti-horse-*SLN* pAb GS3379 detected synthetic horse *SLN* loaded at 2.5–10 ng *SLN* per lane (Figure 2), thereby validating pAb GS3379 as an avid antibody for detection of horse *SLN*.

Per immunoblotting of horse SR vesicles, anti-horse-*SLN* pAb GS3379 showed a small amount of detection of native *SLN* expression in horse SR vesicles (10KP fraction), when horse SR vesicles were when loaded at 10  $\mu$ g SR protein per lane, albeit at a lower intensity level compared to 10 ng of synthetic horse *SLN* (Figure 2). Thus, pAb GS3379 indicates that the *SLN* peptides comprises  $< 0.1\%$  of the total protein in horse SR vesicles. In comparison to synthetic horse *SLN* standard, immunoblot analysis of four horse SR preps using pAb GS3379 determined that native *SLN* is expressed at  $0.16 \pm 0.015$  nmol *SLN*/mg SR protein (Figure 2). The expression level of SERCA in horse SR is estimated at  $\sim 2.1$  nmol SERCA/mg SR protein, per content assessed by Coomassie densitometry and immunoblotting [58], using rabbit SR vesicles as a relative standard with 5.0–6.4 nmol SERCA/mg SR protein [78–80]. Thus, immunoblotting using the anti-horse-*SLN* pAb 3379, with synthetic horse *SLN* peptide as quantitative standard, determined that SR vesicles from horse gluteal muscle express a minor stoichiometric

ratio of ~0.06 SLN/SERCA (mol/mol), i.e., there are ~16 SERCA molecules per available SLN subunit. Since the binding affinity of SLN-SLN self-association is similar to SLN-SERCA regulatory complex formation [81,82], thereby depleting the availability of inhibitory SLN monomers, we conclude that horse SR expresses a large majority of SERCA as SLN-free pumps.

On immunoblots, the small amount of horse SLN in native SR vesicles migrates as a monomer on SDS-PAGE (Figures 2, 3 and S2), as is typically found for rabbit SLN in SR vesicles, and also other SLN orthologs in species-specific SR vesicles, e.g., mouse, dog, and pig [15,17,83,84]. On the other hand, purified SLN (native, recombinant, or synthetic) on SDS-PAGE migrates occasionally as a mix of oligomeric species: abundantly-populated monomers with a variable amount of dimers, and sometimes with lowly-populated trimers and/or tetramers [18,34,85–87] (Figures 2, 3 and S2). Thus, denaturing SDS-PAGE maintains a variable amount of self-association for purified SLN.

Further attempts to detect SLN in horse and rabbit muscle utilized additional commercial and custom-made anti-SLN antibodies. Horse SLN shows sequence divergence and a 1-residue deletion ( $\Delta S4$ ) at the N-terminus, plus a 1-residue deletion ( $\Delta Y30/31$ ) at the C-terminus. The commercial anti-rabbit/mouse/human-SLN pAb ABT13, with immunogen comprising the consensus C-terminus of SLN (residues <sup>27</sup>RSYQY<sup>31</sup>), successfully detected SLN expression in rabbit SR (0.5  $\mu$ g SR protein/lane), but pAb ABT13 did not detect SLN in horse SR (10  $\mu$ g SR protein/lane) (Figure 3). The custom anti-rabbit/mouse/human-SLN pAb PFD-1 generated by Desmond et al., with immunogen comprising a 7-residue stretch of the consensus C-terminus of SLN (residues <sup>25</sup>LVRSYQY<sup>31</sup>) [70], successfully detected rabbit SLN expression in SR vesicles (0.1  $\mu$ g SR protein/lane) and also synthetic rabbit SLN (0.01  $\mu$ g SLN/lane), but pAb PFD-1 did not detect horse SLN in gluteal SR vesicles (10  $\mu$ g SR protein/lane) nor synthetic horse SLN (25 ng SLN/lane) (Figure S2). The commercial pAb 18-395-1-AP, with immunogen comprising human SLN (residues 1–31), did not detect SLN in rabbit SR (0.5  $\mu$ g SR protein/lane) or horse SR (10  $\mu$ g SR protein/lane) (Figure S1). In our assessment, the custom anti-horse-SLN pAb GS3379 gives suitable and reproducible immunoblot results for detecting horse SLN. Furthermore, the commercial anti-rabbit/mouse/human-SLN pAb ABT13 and the custom anti-rabbit/mouse/human-SLN pAb PFD-1, provided by Bloch lab [11,70], both give suitable and reproducible immunoblot results for detecting rabbit SLN. The use of multiple custom and commercial antibodies showed minimal-to-no expression of the SLN peptide in horse SR vesicles.

### 3.5. Correlation of Gene and Protein Expression of SLN in Horse and Rabbit Muscle

When correlating the gene expression of *SLN* versus the protein expression of SLN in horse muscle (normalized per *ATP2A1* and *SERCA1*, respectively), we determined that the high level of *SLN* RNA, with *SLN/ATP2A1* =  $38 \pm 11$  (TPM/TPM) (Figure 1E), produces an insignificant amount of SLN regulatory peptide, with a protein expression ratio of SLN/SERCA ~0.06 (mol/mol) (Figure 2). Thus, the RNA/RNA expression ratio of *SLN/ATP2A* is ~600 fold greater than the protein/protein expression ratio of SLN/SERCA in horse muscle. In comparison, rabbit skeletal muscle shows a relative gene expression ratio of *SLN/ATP2A1* =  $3.1 \pm 0.2$  (TPM/TPM) (Figure 1E) and a protein expression ratio of 0.75–1.2 SLN/SERCA (mol/mol) [18,84], which produces a ~3-fold greater level of RNA/RNA vs. protein/protein expression ratio for SLN/SERCA1. Thus, horse muscle lacks a positive correlation of gene and protein expression levels for SLN and SERCA, unlike rabbit muscle.

### 3.6. Horse Gluteus Expresses A Minimal Level of PLN Inhibitory Peptide Compared to SERCA Protein

Horse muscle expresses a minor level of *PLN* transcripts (Figure 1B). To determine if PLN peptide expression correlates with *PLN* gene transcription, immunoblotting was used to quantitate the expression level of native PLN peptide in horse muscle (Figure 4). The commercial anti-PLN mAb 2D12 recognizes an identical N-terminal sequence among horse and rabbit peptides and has been used effectively in multiple types of experiments: immunoblotting, ELISA, and histochemistry, plus functional assays to disrupt PLN inhibition of SERCA in SR vesicles and live cells [74,88–90]. Quantitative immunoblotting with anti-PLN mAb 2D12 and a synthetic PLN peptide standard

determined that SR vesicles from horse gluteal muscle expresses  $<0.01$  PLN/SERCA (mol/mol) (Figure 4), consistent with previous reports showing low to undetectable level of PLN protein in rabbit muscle [15,91]. The binding affinity of the inhibitory PLN monomer to SERCA is 7-40-fold lower than the binding affinity of PLN monomers in the competing self-association of PLN into non-inhibitory homo-pentamers [92], thereby reducing greatly the available amount of regulatory PLN monomers ( $\ll 0.01$  mol/mol SERCA). We conclude that the PLN peptide in SR vesicles from horse gluteal muscle is expressed at an insignificant level compared to the expression level of SERCA protein.

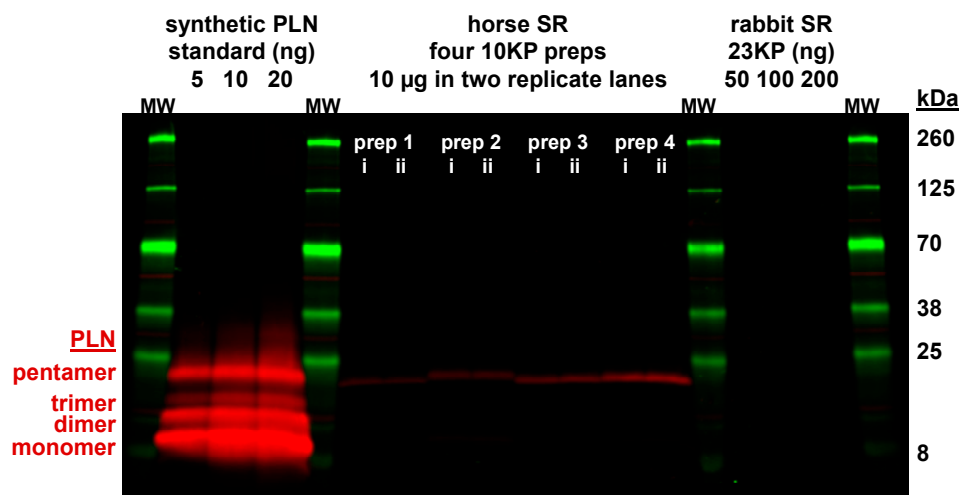


**Figure 4.** Immunoblot analysis using anti-universal-PLN mAb 2D12 detects minimal expression of PLN protein in horse and rabbit SR vesicles. The primary antibody was the commercial anti-PLN mAb 2D12 with epitope  ${}^7\text{LTRSAAIR}^{13}$ , a sequence which is identical in the three PLN orthologs: horse, horse, and rabbit. Samples were electrophoresed through a 4–20% Laemmli gel. Horse SR vesicles ( $N = 4$  preps;  $10 \mu\text{g}$  protein per lane; each prep run in duplicate lanes) and rabbit SR vesicles (50, 100, 200 ng) were assayed. Synthetic human PLN (5, 10, 20 ng) was used as a quantitative standard. Immunoblotting was performed using mAb 2D12 (primary) and goat anti-mouse-IgG pAb labeled with a 680-nm fluorophore (secondary). Immunolabeling was quantified using the LI-COR laser scanner system. Protein gel markers (kDa) are indicated on the right. The proposed molecular species of PLN (monomer, dimer, trimer, and pentamer) on SDS-PAGE are indicated on the left.

#### 4. Discussion

This study is a comparative assessment of gene and protein expression of peptides regulating SERCA  $\text{Ca}^{2+}$  transport in horse and rabbit muscles, thereby providing fundamental information on  $\text{Ca}^{2+}$  regulation at the molecular level. We determined that the horse and rabbit skeletal muscles examined were predominantly composed of fast-twitch fibers expressing *ATP2A1* (SERCA1) and therefore were suitable for comparison [15]. We propose that horse muscle utilizes translational and/or degradation mechanism to mediate a low level of SLN protein expression, and that the high level of *SLN* RNA may possess a cellular function besides translation. The generated results provide new insights into  $\text{Ca}^{2+}$  transport regulation in horse muscle, and a cautionary tale about inferring protein expression level from gene expression analysis.

##### 4.1. Gel analysis for Oligomerization of Horse and Rabbit SLN

On immunoblots, the minimal amount of horse SLN in native SR vesicles migrated as a monomer on SDS-PAGE (Figures 2, 3 and S2), as is typically found for rabbit SLN expressed in SR vesicles, and also other orthologs (mouse, dog, and pig) in respective SR vesicles [15,17,83,84]. Conversely, purified SLN (native, recombinant, or synthetic) on SDS-PAGE migrates often as a mix of oligomeric species: abundantly-populated monomers, a variable amount of dimers, and sometimes with lowly-populated trimers and/or tetramers [18,34,85–87] (Figures 2 and S2). Higher-order oligomers of SLN in SR

are proposed to play key roles in SERCA regulation, as SLN oligomerization competes directly with the binding of inhibitory SLN monomers to SERCA [34,81,86,93,94]. A similar competition of peptide–pump interactions has been well characterized for the PLN–SERCA system, whereby PLN self-association into pentamers competes with the assembly of a PLN monomer and SERCA monomer into an inhibitory hetero–dimeric complex, with the avidity depending on a competing binding equilibria that are dynamically controlled by PLN phosphorylation and SERCA Ca<sup>2+</sup> binding [67,95,96]. Oligomerization of synthetic horse SLN on SDS-PAGE suggests that self-association of horse SLN plays a role in the availability of SLN monomers for inhibition of horse SERCA. Binding of SLN and SERCA in a multimeric, pea-pod complex (SLN monomer, SLN pentamer, and SERCA monomer) is proposed to be an activating mechanism for the Ca<sup>2+</sup> activated ATPase function of SERCA [97].

#### 4.2. Positive and Negative Correlations of Gene Transcription and Protein Expression of SR Ca<sup>2+</sup> Transport Regulators in Horse Gluteal Muscle

Transcriptome sequencing is a powerful tool for identifying gene transcription and changes that occur during physiologic or pathologic perturbations. In our study we found that horses have exceptionally high *SLN* transcription relative to other regulatory peptides (*PLN*, *MRLN*, *DWOLF*) and SERCA genes (*ATP2A1*, *ATP2A2*, *ATP2A3*). These relative expression levels are consistent with qPCR analyses that determined the *SLN* gene (versus *PLN*, *MRLN* or *DWOLF*) is the predominant regulatory peptide transcript expressed in the middle gluteal muscle of Thoroughbred horses [32]. mRNA transcript abundance is often used, and can be, an excellent proxy for protein level in terms of whether or not a specific protein is expressed within specific tissues [98,99]. To infer more exact cellular concentration of proteins is imprecise because on average protein level correlates with the abundance of corresponding mRNA with a squared Pearson correlation coefficient of 0.40 [100]. Stronger positive correlation for Ca<sup>2+</sup> regulatory transcript abundance and protein expression, however, has been shown in a mouse microarray-proteomic study that included calsequestrin (*CASQ2*  $r = 0.999893$ ) and the sodium/potassium-transporting ATPase catalytic subunit (*ATP1A1*  $r = 0.901647$ ) [101]. Vangheluwe et al. found that *SLN* mRNA expression in skeletal muscle correlates positively to SLN peptide expression in mouse, rat, rabbit, and pig skeletal muscle [15]. Previous work has shown also that SLN peptide expression correlates with *SLN* mRNA transcription in mouse leg muscle [102].

To detect horse SLN in horse gluteal muscle, we tested commercial and custom-made antibodies. The pAb ABT13, with immunogen the consensus C-terminus of SLN (<sup>27</sup>RSYQY<sup>31</sup>), showed little to no immunoreactivity for SLN in horse SR vesicles, yet pAb ABT13 identified successfully SLN in rabbit SR vesicles (Figure 3). Our custom anti-horse-SLN pAb GS3379 was successful in detecting synthetic horse SLN; this custom pAb detected minimal levels of SLN expressed in horse SR vesicles (Figure 2). Thus, correlating *SLN* gene expression with SLN protein expression, we found that the high level of *SLN* RNA transcripts in horse muscle do not result in significant SLN protein production. The protein expression ratio of SLN/SERCA was ~0.06 (mol/mol) for horse compared to 0.75 or 1.2 SLN per SERCA (mol/mol) rabbit skeletal muscle [18,84]. Thus, it was quite remarkable that, in spite of mRNA abundance, our immunoblotting results demonstrated an insignificant expression of SLN in horse SR compared to SERCA.

In addition, gene and protein expression of the SERCA inhibitor PLN was negligible in horse muscle with a ratio of <0.01 PLN/SERCA (mol/mol) (Figure 4). Also, minimal gene transcription was found for *MRLN* and *DWOLF* (Figure 1). Thus, our results suggest that horse gluteus is a native adult mammalian muscle that shows insignificant-to-undetectable expression of the most-common regulatory peptides of SERCA (e.g., SLN, PLN, and MRLN). We acknowledge that additional research is needed to support this claim.



#### 4.3. Is There a Mammalian Striated Muscle Reported to Expresses SERCA in the Absence of Regulatory Transmembrane Peptide?

The long-held traditional view on  $\text{Ca}^{2+}$  regulation in striated muscles (skeletal and cardiac) has been that in each specific myocyte type, SERCA is co-expressed with one specific regulatory transmembrane peptide (either SLN or PLN or MLRN) to produce a reversible inhibitory interaction, forming an heterodimeric complex whereby SERCA activity is inhibited until post-translational modification of the regulatory peptide subunit occurs (for review, see Primeau et al. [103]). More recently, there have been reports of three-way co-expression of SERCA, SLN, and PLN together, as assessed at the single-cell level, in human leg postural muscle (vastus lateralis) and Takotsubo cardiomyopathy patients (left ventricle), with enhanced SERCA inhibition [16,104]. These results support MacLennan's seminal report of "super-inhibitory" trimeric complexes comprising one catalytic pump (SERCA) and two inhibitory subunits (SLN and PLN), proposed to be expressed in native muscle and heart [105,106], as initially assessed via cell culture and mouse models of epitope-tagged peptide regulators. As additional peptide regulators of SERCA continue to be identified, the gene/peptide family has been termed "regulins" [13,82,103,107,108].

It is becoming clear that SERCA and its regulatory peptides are expressed broadly in tissue-specific patterns, with concomitant single and dual physiological coupling to SERCA [16,70,105,109]. In mouse slow-twitch muscle, genetic knock-out of SLN expression results in enhanced ATP-dependent  $\text{Ca}^{2+}$  uptake by SERCA [110]. In patients with atrial fibrillation, or heart failure with preserved ejection fraction, decreased expression of SLN correlates with increased  $\text{Ca}^{2+}$  uptake in atrial homogenates; however, it is unknown whether decreased SLN inhibition and subsequent SERCA activation are *compensatory* or *causative* in disease progression [111,112]. It is possible that the *Equus* species evolved a genetic short-cut for speed to evade predators whereby a unique SLN peptide sequence and minimal expression level leaves SERCA function uninhibited, thereby providing rapid relaxation and enhanced contractility for the next muscle contraction. We identified a surprising disconnection between the supra-abundant transcription of *SLN* mRNA from significant expression of the SLN protein. We propose that horse muscle utilizes translational and/or degradation mechanisms to mediate a low basal level of SLN protein, and that the high level of *SLN* RNA may possess a cellular function besides translation.

#### 4.4. Does the *SLN* Gene Transcript Act as A Functional Long Non-Coding RNA for Controlling Contractility of Horse Gluteal Muscle?

Transcriptional regulation is the primary mechanism for the control of eukaryotic protein expression, yet throttling of protein translation from mRNA is also common, including effects by encumbered 5' noncoding sequences, regulation by micro-RNAs, and accessory proteins binding to mRNA or ribosomes [113]. At first, our unique detection of the dissociation between *SLN* RNA and SLN protein levels in horse muscle seemed surprising (Figures 1–3 and S2). However, there is precedence in the literature.

(i) The *MLRN* RNA transcript was first identified as a functional lncRNA (*Linc-RAM*) that modulates myogenic differentiation in mice [114,115]. The *Linc-RAM* RNA was later found to serve also as a translated mRNA that encodes the 36-residue peptide MLRN that inhibits SERCA in mouse muscle [10,82]. Thus, it is possible that transcription and translation of *SLN* acts as key control mechanisms for the regulation of muscle development and contractility.

(ii) Human airway smooth muscle cells express abundant *PLN* RNA but do not express PLN protein [116]. Assays in this study included immunoblotting and immunoprecipitation of human airway smooth muscle homogenates, and immunohistochemistry of enzymatically isolated human airway smooth muscle myocytes. These antibody-based approaches were corroborated by functional assay of cultured human airway smooth muscle cells, whereby siRNA-*PLN*-knockdown had no effect on SR  $\text{Ca}^{2+}$  uptake in live cells or culture homogenates [116]. Similarly, our preliminary functional assays indicated that SLN protein is minimally expressed in horse gluteus muscle, since the anti-horse-SLN pAb 3379 has no effect on  $\text{Ca}^{2+}$  transport by SR vesicles from horse gluteal muscle, consistent with the

lack of SLN protein expression (data not shown). These results indicate that the small level of SLN peptide expression detected in horse SR (~1 SLN molecule per 13–16 SERCA molecules) has a minimal effect on the regulation of SERCA activity in gluteal myocytes in vivo.

In addition, recent articles report transcriptional, translational, and protein degradation mechanisms whereby lncRNA regulate the expression of regulin-type inhibitory peptides and the activity of SERCA Ca<sup>2+</sup> pumps in striated muscles. Here we describe newly proposed molecular mechanisms that may provide analogous insights into the high level of *SLN* gene expression and the low level of SLN peptide expression in horse muscle.

(i) The lncRNA *ZFAS1* in mouse heart is proposed to be a dual-mode inhibitor of SERCA that acts by (a) decreasing *ATP2A2* gene expression and (b) directly inhibiting SERCA2a enzyme activity [117]. Thus, *ZFAS1* lncRNA decreases the quantity and quality of Ca<sup>2+</sup> transport in mouse SR. Analogously, we suggest the possibility that the high level of *SLN* RNA (sans SLN peptide) in horse gluteal muscle acts to regulate gene expression and/or activity of Ca<sup>2+</sup> regulatory protein(s), including SERCA as a potential target. Indeed, *ZFAS1* lncRNA inhibits SERCA2a activity in vitro and in live cardiomyocytes, and over-expression of *ZFAS1* RNA in mouse left ventricle induces cardiac hypertrophy and ultimately heart failure [117].

(ii) The Veglia lab has demonstrated that random-sequence short RNAs, random-sequence single-stranded DNA oligonucleotides, and microRNAs #1 and #9 all bind the PLN peptide, thereby acting to relieve PLN inhibition of SERCA [118,119]. Thus, these recent studies indicate that nucleic acids show the potential to regulate a variety of central cellular functions through key molecular mechanisms, including Ca<sup>2+</sup> regulation as a checkpoint hub. Indeed, there may be a species-specific array of currently unidentified lncRNA that act in distinct roles to regulate myofiber contractility and muscle adaptation in health and disease.

(iii) Hundreds of additional lncRNA with sORF (e.g., between 99 and 300 nucleotides) in human heart are reported to be translated as a peptide/small protein comprising 33 to 100 residues (also known colloquially as “micropeptide” or “microprotein”), including SR-targeted peptides that may act as regulators of cardiac contractility and development [120]. Thus, lncRNA may switch between functional modes: non-coding, or coding, or both.

#### 4.5. Potential Mechanisms to Control SLN Protein Expression and SERCA Regulation in Horse Gluteal Muscle

In addition to the discussed possible mechanisms of direct control, there may be additional mechanisms by which the protein expression and targeting of the gene family of regulin-type peptides and SERCA proteins are controlled.

(i) Chaperone activity of SLN peptides in horse muscle. It is possible that SLN functions as a chaperone to target SERCA1 to longitudinal SR of skeletal muscle myofibers. For example, sAnk1 is peptide (non-regulin family member) that acts to help target SERCA1 to longitudinal SR and to maintain the ultrastructure of longitudinal SR of mouse myofibers [121]; in addition, sAnk1 also acts as a regulin-like peptide inhibitor of SERCA1 activity in a heterologous expression system [11,70]. On the other hand, the SERCA2 protein contributes to targeting PLN to longitudinal SR of cardiomyocytes, via the newly-identified NEST pathway (nuclear ER to SR via T-tubule transit), as reported by Cala and Chen [122,123]. Similarly, SERCA1 contributes to targeting SLN peptides to endoplasmic reticulum of cultured human embryonic kidney cells [35,36,124].

(ii) Degradation of SLN peptides in horse muscle. The peptide expression of PLN, the SLN-analog in ventricular and slow-twitch skeletal muscles, is controlled by multiple mechanisms. In the heart, PLN peptides are reported to be selectively degraded (relative to SERCA proteins) by a metformin-induced ubiquitin-mediated pathway and a phosphorylation-induced autophagy-mediated pathway [125,126]. In testes, PLN peptides are reported to be degraded by intramembrane proteolysis [108,127]. Thus, it is possible that horse muscle utilizes similar mechanism(s) for robust degradation of SLN peptides that are translated from the abundant level of *SLN* RNA transcripts.

(iii) RNA control of *SLN* transcription and translation in horse muscle. Micro-RNAs control transcription and translation of key targets (i.e., mRNAs, lncRNAs, and proteins) in numerous organisms and cell types [128–130]. Thus, it is possible that micro-RNAs in horse gluteal muscle act to shut down *SLN* peptide production from the high-level of *SLN* transcript production.

(iv) Control of SERCA protein degradation in horse muscle. The lncRNA *DACH1* is reported to directly bind and increase ubiquitination of SERCA2 in heart failure, thereby enhancing SERCA protein degradation, decreasing SR  $\text{Ca}^{2+}$  re-uptake, and inhibiting cardiac contractility [131]. It is possible that horse gluteal muscle has dynamically-regulated mechanisms to control the rate of SERCA1a degradation.

We propose that lncRNA help mediate the control of the steady-state level of cellular proteins that regulate  $\text{Ca}^{2+}$  homeostasis in horse gluteal muscle, using multiple mechanisms: transcription, translation, and degradation. Thoroughbred horses with recurrent exertional rhabdomyolysis (RER) have 50% faster relaxation times than horses that are not predisposed to recurrent exertional rhabdomyolysis [132]. It is possible that the defect in abnormal regulation of muscle contraction proposed to be the basis for recurrent exertional rhabdomyolysis arises from abnormal regulation of the steady state level of muscle proteins involved in  $\text{Ca}^{2+}$  regulation.

#### 4.6. Study Limitations

Ideally, our transcriptomic analysis would have been performed in the same horses as *SLN* immunoblotting. We took advantage, however, of transcriptomic data already generated at considerable expense in Arabian horses, and we confirmed similar expression of *SLN*, *PLN*, *MRLN*, *DWOLF*, and *ATP2A1* in the transcriptome of Warmblood horses (data not shown). Due to the large amount of muscle required to isolate a sufficient amount of SR vesicles to perform thorough biochemical analyses, euthanasia is required, and thus donated horses comprised the more common Quarter Horse and Thoroughbred breeds. We have also reported that the unique *SLN* sequence is identical across equine breeds such as Quarter Horse, Standardbred, Thoroughbred, Przewalski Horse, Zebra, and Donkey [32], therefore indicating that the breed differences of samples used in the present study did not have a major impact on our findings. Thus, we propose that quantitative comparison of gene and protein expression levels among different horse breeds is valid analytically.

## 5. Summary

The inhibitory functions of *SLN* on SERCA activity are clear *in vitro*. *SLN* gene expression and protein levels are increased many-fold in standard mouse models of Duchenne's muscular dystrophy, e.g., *mdx* and *mdx/utr-dko* [111]. In compelling mouse and canine models of muscle disease, reducing *SLN* protein expression has been proposed to be an effective therapy [133]. However, decreasing *SLN* expression in alternative mouse models is reported to have beneficial or deleterious effects, depending on the genetic model and etiology studied [133–135]. To help delineate these disparate effects, additional correlations should be determined between  $\text{Ca}^{2+}$  transport regulation and muscular performance in large-animal models which may then provide insights into species-specific adaptations to enhance muscle contraction. Such studies could potentially impact therapeutic control of animal and human muscle disease. We suggest that further investigation is needed to define these pathways per species, muscle-type, and health status.

Our integrative transcriptional and biochemical methodologies provide novel information on gene and protein expression in horse SR, which is a unique physiological system for high-capacity  $\text{Ca}^{2+}$  transport. In horse gluteal muscle, we made two observations that were surprising: (i) *SLN* and *PLN* proteins were detected at miniscule levels in horse SR, i.e., SERCA is apparently unregulated by inhibitory transmembrane peptides in equine skeletal muscle, and (ii) the supra-abundant transcription of *SLN* mRNA is disconnected from stable expression of *SLN* protein. Data reported here contribute to the understanding of  $\text{Ca}^{2+}$  cycling in horse myofibers, with relevance to evolutionary development. Our ongoing functional studies continue to determine mechanistic roles of SERCA, *SLN*, CASQ, and

RYR activities in horse muscle contractility, including the correlation of gene expression, protein homeostasis, and enzyme activity levels. We propose that experimental and computational analyses of the  $\text{Ca}^{2+}$  regulatory system in horse SR will enhance basic understanding of potential therapeutic targets to modulate muscle  $\text{Ca}^{2+}$  homeostasis.

**Supplementary Materials:** The following two Supplementary Figures are available online at MDPI *Veterinary Sciences*, <http://www.mdpi.com/2306-7381/7/4/178/s1>; Figure S1: Immunoblot analysis using anti-human-SLN pAb 18395-1-AP detects minimal expression of SLN protein in horse and rabbit SR vesicles, and Figure S2: Immunoblot analysis using custom anti-rabbit/mouse/human-SLN pAb PFD-1 identifies SLN protein expression in rabbit SR vesicles, but not in horse SR.

**Author Contributions:** Conceptualization, J.M.A., D.D.T., and S.J.V.; Data curation, J.M.A., C.B.K., S.P. and S.J.V.; Formal analysis, J.M.A., C.B.K., S.P., C.J.F. and S.J.V.; Funding acquisition, J.M.A., E.C.M., D.D.T. and S.J.V.; Investigation, J.M.A., C.B.K., S.P., E.C.M. and S.J.V.; Methodology, J.M.A., C.B.K., C.J.F. and S.J.V.; Project administration, J.M.A., E.C.M., D.D.T. and S.J.V.; Resources, J.M.A., C.B.K., C.J.F., D.D.T. and S.J.V.; Supervision, J.M.A., D.D.T. and S.J.V.; Validation, J.M.A., C.B.K. and S.J.V.; Visualization, J.M.A., C.B.K. and S.J.V.; Writing—original draft, J.M.A. and S.J.V.; Writing—review and editing, J.M.A., S.P., C.J.F., E.C.M., D.D.T. and S.J.V. All authors have read and agreed to the published version of the manuscript.

**Funding:** Research reported in this publication was supported in part by the Morris Animal Foundation under award number D16EQ-004 to S.J.V., J.M.A., and D.D.T., plus award number D14EQ-021 to E.C.M. and S.J.V. Morris Animal Foundation is the global leader in supporting science that advances animal health. Research reported in this publication was supported in part by the National Institutes of Health under award numbers R01GM027906, R01HL139065, and R37AG026160 to D.D.T. The content of this publication is solely the responsibility of the authors and does not necessarily represent the official views of the National Institutes of Health. The funding agencies had no role in study design, data collection, data analysis, manuscript preparation, or decision to publish.

**Acknowledgments:** We thank Patrick F. Desmond and Robert L. Bloch for providing the anti-mouse/rabbit/human-SLN polyclonal antibody; Kevin L. Campbell and Bengt Svensson for insightful discussion; Samantha Yuen for technical support; and Octavian Cornea, Destiny Ziebol, and Sarah Blakely Anderson for administrative support. RNA sequencing was performed by the University of Minnesota Genomics Center.

**Conflicts of Interest:** The authors declare that they have no competing interests with the contents of this article. S.J.V. is part-owner of the license for genetic testing of equine type 1 polysaccharide storage myopathy, glycogen branching enzyme deficiency, receiving sales income from their diagnostic use. S.J.V. also receives royalties from the sale of Re-Leve equine feed. The financial and business interests of S.J.V. have been reviewed and managed by Michigan State University in accordance with MSU conflict of interest policies. D.D.T. holds equity in and serves as an executive officer for Photonic Pharma, L.L.C. The financial and business interests of D.D.T. have been reviewed and managed by the University of Minnesota in accordance with UMN conflict of interest policies. Photonic Pharma, L.L.C., had no role in this study.

## Acronyms and Abbreviations

*ATP2A1*, gene encoding SERCA1 protein isoforms; *ATP2A2*, gene encoding SERCA2 protein isoforms; *ATP2A3*, gene encoding SERCA3 protein isoforms; CASQ, calsequestrin; DWORF, dwarf open reading-frame peptide; *g*, gravitational force of 9.8 m/s<sup>2</sup>, defined at average Earth surface level; GP, glycogen phosphorylase; IU, international unit of enzyme activity, defined as the production of 1  $\mu\text{mol}$  product per milligram protein per minute;  $K_{\text{Ca}}$ , apparent  $\text{Ca}^{2+}$  dissociation constant, defined as the  $\text{Ca}^{2+}$  concentration required for half-maximal activation of SERCA activity; lncRNA, long non-coding RNA; mAb, monoclonal antibody; MRLN, myoregulin; pAb, polyclonal antibody; PLN, phospholamban; qRT-PCR, mRNA quantitation using real-time reverse transcription polymerase chain reaction; RER, recurrent exertional rhabdomyolysis; RNA-seq, whole transcriptome shotgun sequencing; RYR, ryanodine receptor  $\text{Ca}^{2+}$  release channel; SERCA, sarco/endoplasmic reticulum  $\text{Ca}^{2+}$ -transporting ATPase; SLN, sarcolipin; sORF, small open reading frame; SR, sarcoplasmic reticulum; TPM, transcripts per million reads;  $V_{\text{max}}$ , maximal enzyme velocity of SERCA, defined as  $\text{Ca}^{2+}$ -activated ATPase activity at saturating concentration of ionized  $\text{Ca}^{2+}$  ( $\sim 5 \mu\text{M}$ ) and  $\text{Mg}\bullet\text{ATP}$  ( $\sim 5 \text{mM}$ ).

## References

1. Nissen, P. Jens Christian Skou (1918–2018). *Science* **2018**, *361*, 133.
2. Møller, J.V.; Olesen, C.; Winther, A.-M.L.; Nissen, P. The sarcoplasmic  $\text{Ca}^{2+}$ -ATPase: Design of a perfect chemi-osmotic pump. *Q. Rev. Biophys.* **2010**, *43*, 501–566. [[CrossRef](#)] [[PubMed](#)]
3. MacLennan, D.H. Isolation of proteins of the sarcoplasmic reticulum. *Methods Enzymol.* **1974**, *32*, 291–302. [[CrossRef](#)] [[PubMed](#)]



4. Tada, M.; Kirchberger, M.A.; Katz, A.M. Phosphorylation of a 22,000-dalton component of the cardiac sarcoplasmic reticulum by adenosine 3':5'-monophosphate-dependent protein kinase. *J. Biol. Chem.* **1975**, *250*, 2640–2647. [[PubMed](#)]
5. Wegener, A.D.; Simmerman, H.K.; Lindemann, J.P.; Jones, L.R. Phospholamban phosphorylation in intact ventricles. Phosphorylation of serine 16 and threonine 17 in response to beta-adrenergic stimulation. *J. Biol. Chem.* **1989**, *264*, 11468–11474. [[PubMed](#)]
6. Bhupathy, P.; Babu, G.J.; Ito, M.; Periasamy, M. Threonine-5 at the N-terminus can modulate sarcolipin function in cardiac myocytes. *J. Mol. Cell. Cardiol.* **2009**, *47*, 723–729. [[CrossRef](#)]
7. Montigny, C.; Decottignies, P.; Le Maréchal, P.; Capy, P.; Bublitz, M.; Olesen, C.; Møller, J.V.; Nissen, P.; Le Maire, M. S-Palmitoylation and S-Oleoylation of Rabbit and Pig Sarcolipin. *J. Biol. Chem.* **2014**, *289*, 33850–33861. [[CrossRef](#)]
8. Sivakumaran, V.; Stanley, B.A.; Tocchetti, C.G.; Ballin, J.D.; Caceres, V.; Zhou, L.; Keceli, G.; Rainer, P.P.; Lee, D.I.; Huke, S.; et al. HNO Enhances SERCA2a Activity and Cardiomyocyte Function by Promoting Redox-Dependent Phospholamban Oligomerization. *Antioxid. Redox Signal.* **2013**, *19*, 1185–1197. [[CrossRef](#)]
9. Zhou, T.; Li, J.; Zhao, P.; Liu, H.; Jia, D.; Jia, H.; He, L.; Cang, Y.; Boast, S.; Chen, Y.-H.; et al. Palmitoyl acyltransferase Aph2 in cardiac function and the development of cardiomyopathy. *Proc. Natl. Acad. Sci. USA* **2015**, *112*, 15666–15671. [[CrossRef](#)]
10. Anderson, D.M.; Anderson, K.M.; Chang, C.-L.; Makarewich, C.A.; Nelson, B.R.; McAnally, J.R.; Kasaragod, P.; Shelton, J.M.; Liou, J.; Bassel-Duby, R.; et al. A Micropeptide Encoded by a Putative Long Noncoding RNA Regulates Muscle Performance. *Cell* **2015**, *160*, 595–606. [[CrossRef](#)]
11. Desmond, P.F.; Muriel, J.; Markwardt, M.L.; Rizzo, M.A.; Bloch, R.J. Identification of Small Ankyrin 1 as a Novel Sarco(endo)plasmic Reticulum Ca<sup>2+</sup>-ATPase 1 (SERCA1) Regulatory Protein in Skeletal Muscle\*. *J. Biol. Chem.* **2015**, *290*, 27854–27867. [[CrossRef](#)]
12. Nelson, B.R.; Makarewich, C.A.; Anderson, D.M.; Winders, B.R.; Troupes, C.D.; Wu, F.; Reese, A.L.; McAnally, J.R.; Chen, X.; Kavalali, E.T.; et al. A peptide encoded by a transcript annotated as long noncoding RNA enhances SERCA activity in muscle. *Science* **2016**, *351*, 271–275. [[CrossRef](#)]
13. Anderson, D.M.; Makarewich, C.A.; Anderson, K.M.; Shelton, J.M.; Bezprozvannaya, S.; Bassel-Duby, R.; Olson, E.N. Widespread control of calcium signaling by a family of SERCA-inhibiting micropeptides. *Sci. Signal.* **2016**, *9*, ra119. [[CrossRef](#)]
14. Makarewich, C.A.; Munir, A.Z.; Schiattarella, G.G.; Bezprozvannaya, S.; Raguimova, O.N.; Cho, E.E.; Vidal, A.H.; Robia, S.L.; Bassel-Duby, R.; Olson, E.N. The DWORF micropeptide enhances contractility and prevents heart failure in a mouse model of dilated cardiomyopathy. *eLife* **2018**, *7*, 7. [[CrossRef](#)]
15. Vangheluwe, P.; Schuermans, M.; Zádor, E.; Waelkens, E.; Raeymaekers, L.; Wuytack, F. Sarcolipin and phospholamban mRNA and protein expression in cardiac and skeletal muscle of different species. *Biochem. J.* **2005**, *389*, 151–159. [[CrossRef](#)] [[PubMed](#)]
16. Fajardo, V.A.; Bombardier, E.; Vigna, C.; Devji, T.; Bloemberg, D.; Gamu, D.; Gramolini, A.O.; Quadrilatero, J.; Tupling, A.R. Co-Expression of SERCA Isoforms, Phospholamban and Sarcolipin in Human Skeletal Muscle Fibers. *PLoS ONE* **2013**, *8*, e84304. [[CrossRef](#)] [[PubMed](#)]
17. Babu, G.J.; Bhupathy, P.; Carnes, C.A.; Billman, G.E.; Periasamy, M. Differential expression of sarcolipin protein during muscle development and cardiac pathophysiology. *J. Mol. Cell. Cardiol.* **2007**, *43*, 215–222. [[CrossRef](#)] [[PubMed](#)]
18. Odermatt, A.; Becker, S.; Khanna, V.K.; Kurzydowski, K.; Leisner, E.; Pette, D.; MacLennan, D.H. Sarcolipin Regulates the Activity of SERCA1, the Fast-twitch Skeletal Muscle Sarcoplasmic Reticulum Ca<sup>2+</sup>-ATPase. *J. Biol. Chem.* **1998**, *273*, 12360–12369. [[CrossRef](#)]
19. Smith, W.S. Sarcolipin uncouples hydrolysis of ATP from accumulation of Ca<sup>2+</sup> by the Ca<sup>2+</sup>-ATPase of skeletal-muscle sarcoplasmic reticulum. *Biochem. J.* **2002**, *361*, 277–286. [[CrossRef](#)]
20. Buck, B.; Zmoon, J.; Kirby, T.L.; DeSilva, T.M.; Karim, C.B.; Thomas, D.D.; Veglia, G. Overexpression, purification, and characterization of recombinant Ca-ATPase regulators for high-resolution solution and solid-state NMR studies. *Protein Expr. Purif.* **2003**, *30*, 253–261. [[CrossRef](#)]
21. Espinoza-Fonseca, L.M.; Autry, J.M.; Thomas, D.D. Sarcolipin and phospholamban inhibit the calcium pump by populating a similar metal ion-free intermediate state. *Biochem. Biophys. Res. Commun.* **2015**, *463*, 37–41. [[CrossRef](#)] [[PubMed](#)]



22. Sahoo, S.K.; Shaikh, S.A.; Sopariwala, D.H.; Bal, N.C.; Bruhn, D.S.; Kopec, W.; Khandelia, H.; Periasamy, M. The N Terminus of Sarcolipin Plays an Important Role in Uncoupling Sarco-endoplasmic Reticulum Ca<sup>2+</sup>-ATPase (SERCA) ATP Hydrolysis from Ca<sup>2+</sup>-Transport. *J. Biol. Chem.* **2015**, *290*, 14057–14067. [[CrossRef](#)] [[PubMed](#)]
23. Autry, J.M.; Thomas, D.D.; Espinoza-Fonseca, L.M. Sarcolipin Promotes Uncoupling of the SERCA Ca<sup>2+</sup> Pump by Inducing a Structural Rearrangement in the Energy-Transduction Domain. *Biochemistry* **2016**, *55*, 6083–6086. [[CrossRef](#)]
24. Espinoza-Fonseca, L.M.; Autry, J.M.; Ramírez-Salinas, G.L.; Thomas, D.D. Atomic-Level Mechanisms for Phospholamban Regulation of the Calcium Pump. *Biophys. J.* **2015**, *108*, 1697–1708. [[CrossRef](#)]
25. Gortari, E.F.-D.; Espinoza-Fonseca, L.M. Structural basis for relief of phospholamban-mediated inhibition of the sarcoplasmic reticulum Ca<sup>2+</sup>-ATPase at saturating Ca<sup>2+</sup>-conditions. *J. Biol. Chem.* **2018**, *293*, 12405–12414. [[CrossRef](#)]
26. Campbell, K.L.; Dicke, A.A. Sarcolipin Makes Heat, but Is It Adaptive Thermogenesis? *Front. Physiol.* **2018**, *9*, 714. [[CrossRef](#)]
27. Gramolini, A.O.; Trivieri, M.G.; Oudit, G.Y.; Kislinger, T.; Li, W.; Patel, M.M.; Emili, A.; Kranias, E.G.; Backx, P.H.; MacLennan, D.H. Cardiac-specific overexpression of sarcolipin in phospholamban null mice impairs myocyte function that is restored by phosphorylation. *Proc. Natl. Acad. Sci. USA* **2006**, *103*, 2446–2451. [[CrossRef](#)]
28. Barbot, T.; Montigny, C.; Decottignies, P.; Le Maire, M.; Jaxel, C.; Jamin, N.; Beswick, V. *Functional and Structural Insights into Sarcolipin, a Regulator of the Sarco-Endoplasmic Reticulum Ca<sup>2+</sup>-ATPases*; Chakraborti, S., Dhalla, N.S., Eds.; Springer: Cham, Switzerland, 2016; pp. 153–186.
29. Johnson, C.N.; Pattanayek, R.; Potet, F.; Rebbeck, R.T.; Blackwell, D.J.; Nikolaienko, R.; Sequeira, V.; Le Meur, R.; Radwański, P.B.; Davis, J.P.; et al. The CaMKII inhibitor KN93-calmodulin interaction and implications for calmodulin tuning of NaV1.5 and RyR2 function. *Cell Calcium* **2019**, *82*, 102063. [[CrossRef](#)]
30. McCarthy, M.R.; Savich, Y.; Cornea, R.L.; Thomas, D.D. Resolved Structural States of Calmodulin in Regulation of Skeletal Muscle Calcium Release. *Biophys. J.* **2020**, *118*, 1090–1100. [[CrossRef](#)]
31. Cala, S.E.; Scott, B.T.; Jones, L.R. Intralumenal sarcoplasmic reticulum Ca(2+)-binding proteins. *Semin. Cell Biol.* **1990**, *1*, 265–275. [[PubMed](#)]
32. Valberg, S.J.; Soave, K.; Williams, Z.J.; Perumbakkam, S.; Schott, M.; Finno, C.J.; Petersen, J.L.; Fenger, C.; Autry, J.M.; Thomas, D.D. Coding sequences of sarcoplasmic reticulum calcium ATPase regulatory peptides and expression of calcium regulatory genes in recurrent exertional rhabdomyolysis. *J. Vet. Intern. Med.* **2019**, *33*, 933–941. [[CrossRef](#)] [[PubMed](#)]
33. Gaudry, M.J.; Jastroch, M.; Treberg, J.R.; Hofreiter, M.; Paijmans, J.L.A.; Starrett, J.; Wales, N.; Signore, A.V.; Springer, M.S.; Campbell, K.L. Inactivation of thermogenic UCP1 as a historical contingency in multiple placental mammal clades. *Sci. Adv.* **2017**, *3*, e1602878. [[CrossRef](#)] [[PubMed](#)]
34. Gorski, P.A.; Graves, J.P.; Vangheluwe, P.; Young, H.S. Sarco(endo)plasmic Reticulum Calcium ATPase (SERCA) Inhibition by Sarcolipin Is Encoded in Its Luminal Tail. *J. Biol. Chem.* **2013**, *288*, 8456–8467. [[CrossRef](#)] [[PubMed](#)]
35. Gramolini, A.O.; Kislinger, T.; Asahi, M.; Li, W.; Emili, A.; MacLennan, D.H. Sarcolipin retention in the endoplasmic reticulum depends on its C-terminal RSYQY sequence and its interaction with sarco(endo)plasmic Ca<sup>2+</sup>-ATPases. *Proc. Natl. Acad. Sci. USA* **2004**, *101*, 16807–16812. [[CrossRef](#)] [[PubMed](#)]
36. Butler, J.; Lee, A.G.; Wilson, D.I.; Spalluto, C.; Hanley, N.; East, J.M. Phospholamban and sarcolipin are maintained in the endoplasmic reticulum by retrieval from the ER-Golgi intermediate compartment. *Cardiovasc. Res.* **2007**, *74*, 114–123. [[CrossRef](#)] [[PubMed](#)]
37. Gutiérrez-Martín, Y.; Martín-Romero, F.J.; Iñesta-Vaquera, F.A.; Gutiérrez-Merino, C.; Henao, F. Modulation of sarcoplasmic reticulum Ca<sup>2+</sup>-ATPase by chronic and acute exposure to peroxynitrite. *JBIC J. Biol. Inorg. Chem.* **2004**, *271*, 2647–2657. [[CrossRef](#)]
38. Knyushko, T.V.; Sharov, V.S.; Williams, T.D.; Schöneich, C.; Bigelow, D.J. 3-Nitrotyrosine Modification of SERCA2a in the Aging Heart: A Distinct Signature of the Cellular Redox Environment. *Biochemistry* **2005**, *44*, 13071–13081. [[CrossRef](#)]
39. MacLeay, J.M.; Sorum, S.A.; Valberg, S.J.; Marsh, W.E.; Sorum, M.D. Epidemiologic analysis of factors influencing exertional rhabdomyolysis in Thoroughbreds. *Am. J. Vet. Res.* **1999**, *60*, 1562–1566.

40. Cole, F.L.; Mellor, D.J.; Hodgson, D.R.; Reid, S.W.J. Prevalence and demographic characteristics of exertional rhabdomyolysis in horses in Australia. *Vet. Rec.* **2004**, *155*, 625–630. [[CrossRef](#)]
41. Wilberger, M.S.; McKenzie, E.; Payton, M.E.; Rigas, J.D.; Valberg, S.J. Prevalence of exertional rhabdomyolysis in endurance horses in the Pacific Northwestern United States. *Equine Vet. J.* **2015**, *47*, 165–170. [[CrossRef](#)]
42. Cheng, A.J.; Andersson, D.; Lanner, J.T. Can't live with or without it: Calcium and its role in Duchenne muscular dystrophy-induced muscle weakness. Focus on "SERCA1 overexpression minimizes skeletal muscle damage in dystrophic mouse models". *Am. J. Physiol. Physiol.* **2015**, *308*, C697–C698. [[CrossRef](#)] [[PubMed](#)]
43. Fruen, B.R.; Mickelson, J.R.; Louis, C.F. Dantrolene Inhibition of Sarcoplasmic Reticulum Ca<sup>2+</sup>Release by Direct and Specific Action at Skeletal Muscle Ryanodine Receptors. *J. Biol. Chem.* **1997**, *272*, 26965–26971. [[CrossRef](#)] [[PubMed](#)]
44. Edwards, J.G.T.; Newtont, J.R.; Ramzan, P.H.L.; Pilsworth, R.C.; Shepherd, M.C. The efficacy of dantrolene sodium in controlling exertional rhabdomyolysis in the Thoroughbred racehorse. *Equine Vet. J.* **2003**, *35*, 707–711. [[CrossRef](#)] [[PubMed](#)]
45. McKenzie, E.C.; Valberg, S.J.; Godden, S.M.; Finno, C.J.; Murphy, M.J. Effect of oral administration of dantrolene sodium on serum creatine kinase activity after exercise in horses with recurrent exertional rhabdomyolysis. *Am. J. Vet. Res.* **2004**, *65*, 74–79. [[CrossRef](#)]
46. McDonald, A.G.; Boyce, S.; Tipton, K.F. ExplorEnz: The primary source of the IUBMB enzyme list. *Nucleic Acids Res.* **2009**, *37*, D593–D597. [[CrossRef](#)]
47. Strausberg, R.L. Generation and initial analysis of more than 15,000 full-length human and mouse cDNA sequences. *Proc. Natl. Acad. Sci. USA* **2002**, *99*, 16899–16903.
48. Zhang, Y.; Fujii, J.; Phillips, M.S.; Chen, H.-S.; Karpati, G.; Yee, W.-C.; Schrank, B.; Cornblath, D.R.; Boylan, K.B.; MacLennan, D.H. Characterization of cDNA and Genomic DNA Encoding SERCA1, the Ca<sup>2+</sup>-ATPase of Human Fast-Twitch Skeletal Muscle Sarcoplasmic Reticulum, and Its Elimination as a Candidate Gene for Brody Disease. *Genomics* **1995**, *30*, 415–424. [[CrossRef](#)]
49. Odermatt, A.; Taschner, P.E.M.; Scherer, S.W.; Beatty, B.; Khanna, V.K.; Cornblath, D.R.; Chaudhry, V.; Yee, W.-C.; Schrank, B.; Karpati, G.; et al. Characterization of the Gene Encoding Human Sarcolipin (SLN), a Proteolipid Associated with SERCA1: Absence of Structural Mutations in Five Patients with Brody Disease. *Genomics* **1997**, *45*, 541–553. [[CrossRef](#)]
50. Fujii, J.; Lytton, J.; Tada, M.; MacLennan, D.H. Rabbit cardiac and slow-twitch muscle express the same phospholamban gene. *FEBS Lett.* **1988**, *227*, 51–55. [[CrossRef](#)]
51. Fujii, J.; Zarain-Herzberg, A.; Willard, H.F.; Tada, M.; MacLennan, D.H. Structure of the rabbit phospholamban gene, cloning of the human cDNA, and assignment of the gene to human chromosome 6. *J. Biol. Chem.* **1991**, *266*, 11669–11675.
52. Fujii, J.; Ueno, A.; Kitano, K.; Tanaka, S.; Kadoma, M.; Tada, M. Complete complementary DNA-derived amino acid sequence of canine cardiac phospholamban. *J. Clin. Investig.* **1987**, *79*, 301–304. [[CrossRef](#)] [[PubMed](#)]
53. Sayers, E.W.; Cavanaugh, M.; Clark, K.; Ostell, J.; Pruitt, K.D.; Karsch-Mizrachi, I. GenBank. *Nucleic Acids Res.* **2019**, *48*, D84–D86.
54. Lindholm, A.; Piehl, K. Fibre composition, enzyme activity and concentrations of metabolites and electrolytes in muscles of standardbred horses. *Acta Vet. Scand.* **1974**, *15*, 287–309. [[PubMed](#)]
55. Ablorh, N.-A.D.; Dong, X.; James, Z.M.; Xiong, Q.; Zhang, J.; Thomas, D.D.; Karim, C.B. Synthetic Phosphopeptides Enable Quantitation of the Content and Function of the Four Phosphorylation States of Phospholamban in Cardiac Muscle. *J. Biol. Chem.* **2014**, *289*, 29397–29405. [[CrossRef](#)]
56. Ablorh, N.-A.; Miller, T.; Nitu, F.; Gruber, S.J.; Karim, C.B.; Thomas, D.D. Accurate quantitation of phospholamban phosphorylation by immunoblot. *Anal. Biochem.* **2012**, *425*, 68–75. [[CrossRef](#)]
57. Autry, J.M.; Jones, L.R. High-level coexpression of the canine cardiac calcium pump and phospholamban in Sf21 insect cells. *Ann. New York Acad. Sci.* **1998**, *853*, 92–102. [[CrossRef](#)]
58. Autry, J.M.; Karim, C.B.; Cocco, M.; Carlson, S.F.; Thomas, D.D.; Valberg, S.J. Purification of sarcoplasmic reticulum vesicles from horse gluteal muscle. *Anal. Biochem.* **2020**, *610*, 113965. [[CrossRef](#)]
59. Valberg, S.J.; Perumbakkam, S.; McKenzie, E.C.; Finno, C.J. Proteome and transcriptome profiling of equine myofibrillar myopathy identifies diminished peroxiredoxin 6 and altered cysteine metabolic pathways. *Physiol. Genom.* **2018**, *50*, 1036–1050. [[CrossRef](#)]

60. Leberer, E.; Pette, D. Immunochemical quantification of sarcoplasmic reticulum Ca-ATPase, of calsequestrin and of parvalbumin in rabbit skeletal muscles of defined fiber composition. *Jbic J. Biol. Inorg. Chem.* **1986**, *156*, 489–496. [[CrossRef](#)]
61. Yates, A.D. Ensembl 2020. *Nucleic Acids Res.* **2020**, *48*, D682–D688. [[CrossRef](#)]
62. Patro, R.; Duggal, G.; Love, M.I.; Irizarry, M.I.L.R.A.; Kingsford, C. Salmon provides fast and bias-aware quantification of transcript expression. *Nat. Methods* **2017**, *14*, 417–419. [[CrossRef](#)] [[PubMed](#)]
63. Edgar, R.; Domrachev, M.; Lash, A.E. Gene Expression Omnibus: NCBI gene expression and hybridization array data repository. *Nucleic Acids Res.* **2002**, *30*, 207–210. [[CrossRef](#)] [[PubMed](#)]
64. Ikemoto, N.; Sreter, F.; Gergely, J. Structural features of the surface of the vesicles of FSR—Lack of functional role in Ca<sup>2+</sup> uptake and ATPase activity. *Arch. Biochem. Biophys.* **1971**, *147*, 571–582. [[CrossRef](#)]
65. Karim, C.B.; Zhang, Z.; Thomas, D.D. Synthesis of TOAC spin-labeled proteins and reconstitution in lipid membranes. *Nat. Protoc.* **2007**, *2*, 42–49. [[CrossRef](#)] [[PubMed](#)]
66. Li, J.; James, Z.M.; Dong, X.; Karim, C.B.; Thomas, D.D. Structural and Functional Dynamics of an Integral Membrane Protein Complex Modulated by Lipid Headgroup Charge. *J. Mol. Biol.* **2012**, *418*, 379–389. [[CrossRef](#)] [[PubMed](#)]
67. Autry, J.M.; Jones, L.R. Functional Co-expression of the canine cardiac Ca<sup>2+</sup> pump and phospholamban in *Spodoptera frugiperda* (Sf21) cells reveals new insights on ATPase regulation. *J. Biol. Chem.* **1997**, *272*, 15872–15880. [[CrossRef](#)]
68. Mahaney, J.E.; Autry, J.M.; Jones, L.R. Kinetics Studies of the Cardiac Ca-ATPase Expressed in Sf21 Cells: New Insights on Ca-ATPase Regulation by Phospholamban. *Biophys. J.* **2000**, *78*, 1306–1323. [[CrossRef](#)]
69. Guerrero-Hernandez, A.; Sánchez-Vázquez, V.H.; Martínez-Martínez, E.; Sandoval-Vázquez, L.; Perez-Rosas, N.C.; Lopez-Farias, R.; Dagnino-Acosta, A. Sarco-Endoplasmic Reticulum Calcium Release Model Based on Changes in the Luminal Calcium Content. *Atherosclerosis* **2020**, *1131*, 337–370.
70. Desmond, P.F.; Labuza, A.; Muriel, J.; Markwardt, M.L.; Mancini, A.E.; Rizzo, M.A.; Bloch, R.J. Interactions between small ankyrin 1 and sarcolipin coordinately regulate activity of the sarco(endo)plasmic reticulum Ca<sup>2+</sup>-ATPase (SERCA1). *J. Biol. Chem.* **2017**, *292*, 10961–10972. [[CrossRef](#)]
71. Zaman, J.A.; Harling, L.; Ashrafian, H.; Darzi, A.; Gooderham, N.; Athanasiou, T.; Peters, N.S. Post-operative atrial fibrillation is associated with a pre-existing structural and electrical substrate in human right atrial myocardium. *Int. J. Cardiol.* **2016**, *220*, 580–588. [[CrossRef](#)]
72. Rowland, L.A.; Maurya, S.K.; Bal, N.C.; Kozak, L.; Periasamy, M. Sarcolipin and uncoupling protein 1 play distinct roles in diet-induced thermogenesis and do not compensate for one another. *Obesity* **2016**, *24*, 1430–1433. [[CrossRef](#)] [[PubMed](#)]
73. Lee, C.S.; Dagnino-Acosta, A.; Yarotsky, V.; Hanna, A.; Lyfenko, A.; Knoblauch, M.; Georgiou, D.K.; Poché, R.A.; Swank, M.W.; Long, C.; et al. Ca(2+) permeation and/or binding to CaV1.1 fine-tunes skeletal muscle Ca(2+) signaling to sustain muscle function. *Skelet. Muscle* **2015**, *5*, 4. [[CrossRef](#)] [[PubMed](#)]
74. Sham, J.S.; Jones, L.R.; Morad, M. Phospholamban mediates the beta-adrenergic-enhanced Ca<sup>2+</sup> uptake in mammalian ventricular myocytes. *Am. J. Physiol. Circ. Physiol.* **1991**, *261*, H1344–H1349. [[CrossRef](#)] [[PubMed](#)]
75. Jones, L.R.; Cornea, R.L.; Chen, Z. Close Proximity between Residue 30 of Phospholamban and Cysteine 318 of the Cardiac Ca<sup>2+</sup>Pump Revealed by Intermolecular Thiol Cross-linking. *J. Biol. Chem.* **2002**, *277*, 28319–28329. [[CrossRef](#)] [[PubMed](#)]
76. MacLennan, D.H.; Rice, W.J.; Green, N.M. The Mechanism of Ca<sup>2+</sup>Transport by Sarco(Endo)plasmic Reticulum Ca<sup>2+</sup>-ATPases. *J. Biol. Chem.* **1997**, *272*, 28815–28818. [[CrossRef](#)] [[PubMed](#)]
77. Neumann, J.; Boknik, P.; DePaoli-Roach, A.A.; Field, L.J.; Rockman, H.A.; Kobayashi, Y.M.; Kelley, J.S.; Jones, L.R. Targeted Overexpression of Phospholamban to Mouse Atrium Depresses Ca<sup>2+</sup>Transport and Contractility. *J. Mol. Cell. Cardiol.* **1998**, *30*, 1991–2002. [[CrossRef](#)]
78. Shutova, A.N.; Storey, K.B.; Lopina, O.D.; Rubtsov, A.M. Comparative characteristics of sarcoplasmic reticulum preparations from skeletal muscles of the ground squirrel *Spermophilus undulatus*, rats, and rabbits. *Biochemistry (Moscow)* **1999**, *64*, 1250–1257. [[PubMed](#)]
79. Kumar, S.; Li, C.; Montigny, C.; Le Maire, M.; Barth, A. Conformational changes of recombinant Ca<sup>2+</sup>-ATPase studied by reaction-induced infrared difference spectroscopy. *FEBS J.* **2013**, *280*, 5398–5407. [[CrossRef](#)] [[PubMed](#)]

80. Autry, J.M.; Rubin, J.E.; Svensson, B.; Li, J.; Thomas, D.D. Nucleotide Activation of the Ca-ATPase. *J. Biol. Chem.* **2012**, *287*, 39070–39082. [[CrossRef](#)] [[PubMed](#)]
81. Autry, J.M.; Rubin, J.E.; Pietrini, S.D.; Winters, D.L.; Robia, S.L.; Thomas, D.D. Oligomeric Interactions of Sarcolipin and the Ca-ATPase. *J. Biol. Chem.* **2011**, *286*, 31697–31706. [[CrossRef](#)] [[PubMed](#)]
82. Singh, D.R.; Dalton, M.P.; Cho, E.E.; Pribadi, M.P.; Zak, T.J.; Šeflová, J.; Makarewich, C.A.; Olson, E.N.; Robia, S.L. Newly Discovered Micropeptide Regulators of SERCA Form Oligomers but Bind to the Pump as Monomers. *J. Mol. Biol.* **2019**, *431*, 4429–4443. [[CrossRef](#)] [[PubMed](#)]
83. Toyoshima, C.; Iwasawa, S.; Ogawa, H.; Hirata, A.; Tsueda, J.; Inesi, G. Crystal structures of the calcium pump and sarcolipin in the Mg<sup>2+</sup>-bound E1 state. *Nat. Cell Biol.* **2013**, *495*, 260–264. [[CrossRef](#)] [[PubMed](#)]
84. Butler, J.; Smyth, N.; Broadbridge, R.; Council, C.E.; Lee, A.G.; Stocker, C.J.; Hislop, D.C.; Arch, J.R.; Cawthorne, M.A.; East, J.M. The effects of sarcolipin over-expression in mouse skeletal muscle on metabolic activity. *Arch. Biochem. Biophys.* **2015**, *569*, 26–31. [[CrossRef](#)] [[PubMed](#)]
85. Ohnoki, S.; Martonosi, A. Purification and characterization of the proteolipid of rabbit sarcoplasmic reticulum. *Biochim. Et Biophys. Acta (Bba) Protein Struct.* **1980**, *626*, 170–178. [[CrossRef](#)]
86. Hellstern, S.; Pegoraro, S.; Karim, C.B.; Lustig, A.; Thomas, D.D.; Moroder, L.; Engel, J. Sarcolipin, the Shorter Homologue of Phospholamban, Forms Oligomeric Structures in Detergent Micelles and in Liposomes. *J. Biol. Chem.* **2001**, *276*, 30845–30852. [[CrossRef](#)]
87. Graves, J.P. *Cryo-Electron Microscopy of SERCA Interacting with Oligomeric Phospholamban and Oligomeric Sarcolipin*; University of Alberta: Edmonton, AB, Canada, 2011.
88. Movsesian, M.A.; Karimi, M.; Green, K.; Jones, L.R. Ca(2+)-transporting ATPase, phospholamban, and calsequestrin levels in nonfailing and failing human myocardium. *Circulation* **1994**, *90*, 653–657. [[CrossRef](#)]
89. Chen, Z.; Akin, B.L.; Jones, L.R. Mechanism of Reversal of Phospholamban Inhibition of the Cardiac Ca<sup>2+</sup>-ATPase by Protein Kinase A and by Anti-phospholamban Monoclonal Antibody 2D12. *J. Biol. Chem.* **2007**, *282*, 20968–20976. [[CrossRef](#)]
90. Bai, Y.; Jones, P.P.; Guo, J.; Zhong, X.; Clark, R.B.; Zhou, Q.; Wang, R.; Vallmitjana, A.; Benítez, R.; Hove-Madsen, L.; et al. Phospholamban knockout breaks arrhythmogenic Ca<sup>2+</sup> waves and suppresses catecholaminergic polymorphic ventricular tachycardia in mice. *Circ. Res.* **2013**, *113*, 517–526. [[CrossRef](#)]
91. Jones, L.R.; Field, L.J. Residues 2-25 of phospholamban are insufficient to inhibit Ca<sup>2+</sup> transport ATPase of cardiac sarcoplasmic reticulum. *J. Biol. Chem.* **1993**, *268*, 11486–11488.
92. Kelly, E.M.; Hou, Z.; Bossuyt, J.; Bers, D.M.; Robia, S.L. Phospholamban Oligomerization, Quaternary Structure, and Sarco(endo)plasmic Reticulum Calcium ATPase Binding Measured by Fluorescence Resonance Energy Transfer in Living Cells. *J. Biol. Chem.* **2008**, *283*, 12202–12211. [[CrossRef](#)]
93. Cao, Y.; Wu, X.; Yang, R.; Wang, X.; Sun, H.; Lee, I. Self-assembling Study of Sarcolipin and Its Mutants in Multiple Molecular Dynamic Simulations. *Proteins: Struct. Funct. Bioinform.* **2017**, *85*, 1065–1077. [[CrossRef](#)] [[PubMed](#)]
94. Cao, Y.; Wu, X.; Wang, X.; Sun, H.; Lee, I. Transmembrane dynamics of the Thr-5 phosphorylated sarcolipin pentameric channel. *Arch. Biochem. Biophys.* **2016**, *604*, 143–151. [[CrossRef](#)] [[PubMed](#)]
95. Kimura, Y.; Kurzydowski, K.; Tada, M.; MacLennan, D.H. Phospholamban Inhibitory Function Is Activated by Depolymerization. *J. Biol. Chem.* **1997**, *272*, 15061–15064. [[CrossRef](#)] [[PubMed](#)]
96. Cornea, R.L.; Autry, J.M.; Chen, Z.; Jones, L.R. Reexamination of the Role of the Leucine/Isoleucine Zipper Residues of Phospholamban in Inhibition of the Ca<sup>2+</sup>-Pump of Cardiac Sarcoplasmic Reticulum. *J. Biol. Chem.* **2000**, *275*, 41487–41494. [[CrossRef](#)]
97. Graves, J.P. Interaction of a Sarcolipin Pentamer and Monomer with the Sarcoplasmic Reticulum Calcium Pump, SERCA. *Biophys. J.* **2020**, *118*, 518–531. [[CrossRef](#)]
98. Lu, P.; Vogel, C.; Wang, R.; Yao, X.; Marcotte, E.M. Absolute protein expression profiling estimates the relative contributions of transcriptional and translational regulation. *Nat. Biotechnol.* **2007**, *25*, 117–124. [[CrossRef](#)]
99. Eichenberger, R.M.; Ramakrishnan, C.; Russo, G.; Deplazes, P.; Hehl, A.B. Genome-wide analysis of gene expression and protein secretion of *Babesia canis* during virulent infection identifies potential pathogenicity factors. *Sci. Rep.* **2017**, *7*, 1–14. [[CrossRef](#)]
100. Vogel, C.; Marcotte, E.M. Insights into the regulation of protein abundance from proteomic and transcriptomic analyses. *Nat. Rev. Genet.* **2012**, *13*, 227–232. [[CrossRef](#)]



101. Kislinger, T.; Cox, B.; Kannan, A.; Chung, C.; Hu, P.; Ignatchenko, A.; Scott, M.S.; Gramolini, A.O.; Morris, Q.; Hallett, M.T.; et al. Global Survey of Organ and Organelle Protein Expression in Mouse: Combined Proteomic and Transcriptomic Profiling. *Cell* **2006**, *125*, 173–186. [[CrossRef](#)]
102. Pant, M.; Bal, N.C.; Periasamy, M. Cold adaptation overrides developmental regulation of sarcolipin expression in mice skeletal muscle: SOS for muscle-based thermogenesis? *J. Exp. Biol.* **2015**, *218*, 2321–2325. [[CrossRef](#)]
103. Primeau, J.O.; Armanious, G.P.; Fisher, M.E.; Young, H.S. The SarcoEndoplasmic Reticulum Calcium ATPase. *Subcell. Biochem.* **2018**, *87*, 229–258. [[PubMed](#)]
104. Nef, H.M.; Möllmann, H.; Troidl, C.; Kostin, S.; Voss, S.; Hilpert, P.; Behrens, C.B.; Rolf, A.; Rixe, J.; Weber, M.; et al. Abnormalities in intracellular Ca<sup>2+</sup> regulation contribute to the pathomechanism of Tako-Tsubo cardiomyopathy. *Eur. Hear. J.* **2009**, *30*, 2155–2164. [[CrossRef](#)] [[PubMed](#)]
105. Asahi, M.; Kurzydowski, K.; Tada, M.; MacLennan, D.H.; Čabart, P.; Murphy, S. Sarcolipin Inhibits Polymerization of Phospholamban to Induce Superinhibition of Sarco(endo)plasmic Reticulum Ca<sup>2+</sup>-ATPases (SERCAs). *J. Biol. Chem.* **2002**, *277*, 26725–26728. [[CrossRef](#)] [[PubMed](#)]
106. Asahi, M.; Sugita, Y.; Kurzydowski, K.; De Leon, S.; Tada, M.; Toyoshima, C.; MacLennan, D.H. Sarcolipin regulates sarco(endo)plasmic reticulum Ca<sup>2+</sup>-ATPase (SERCA) by binding to transmembrane helices alone or in association with phospholamban. *Proc. Natl. Acad. Sci. USA* **2003**, *100*, 5040–5045. [[CrossRef](#)] [[PubMed](#)]
107. Gorski, P.A.; Ceholski, D.K.; Young, H.S. Structure-Function Relationship of the SERCA Pump and Its Regulation by Phospholamban and Sarcolipin. *Adv. Exp. Med. Biol.* **2017**, *981*, 77–119. [[PubMed](#)]
108. Young, H.S.; Lemieux, M.J. Regulating the regulator: Intramembrane proteolysis of vesicular trafficking proteins and the SERCA regulator phospholamban. *Embo Rep.* **2019**, *20*. [[CrossRef](#)]
109. Morita, T.; Hussain, D.; Asahi, M.; Tsuda, T.; Kurzydowski, K.; Toyoshima, C.; MacLennan, D.H. Interaction sites among phospholamban, sarcolipin, and the sarco(endo)plasmic reticulum Ca<sup>2+</sup>-ATPase. *Biochem. Biophys. Res. Commun.* **2008**, *369*, 188–194. [[CrossRef](#)]
110. Tupling, A.R.; Bombardier, E.; Gupta, S.C.; Hussain, D.; Vigna, C.; Bloemberg, D.; Quadrilatero, J.; Trivieri, M.G.; Babu, G.J.; Backx, P.H.; et al. Enhanced Ca<sup>2+</sup> transport and muscle relaxation in skeletal muscle from sarcolipin-null mice. *Am. J. Physiol. Physiol.* **2011**, *301*, C841–C849. [[CrossRef](#)]
111. Shanmugam, M.; Molina, C.E.; Gao, S.; Severac-Bastide, R.; Fischmeister, R.; Babu, G.J. Decreased sarcolipin protein expression and enhanced sarco(endo)plasmic reticulum Ca<sup>2+</sup> uptake in human atrial fibrillation. *Biochem. Biophys. Res. Commun.* **2011**, *410*, 97–101. [[CrossRef](#)]
112. Molina, C.E.; Abu-Taha, I.H.; Wang, Q.; Roselló-Díez, E.; Kamler, M.; Nattel, S.; Ravens, U.; Wehrens, X.H.T.; Hove-Madsen, L.; Heijman, J.; et al. Profibrotic, Electrical, and Calcium-Handling Remodeling of the Atria in Heart Failure Patients With and Without Atrial Fibrillation. *Front. Physiol.* **2018**, *9*, 1383. [[CrossRef](#)]
113. Kozak, M. An analysis of vertebrate mRNA sequences: Intimations of translational control. *J. Cell Biol.* **1991**, *115*, 887–903. [[CrossRef](#)] [[PubMed](#)]
114. Yu, X.; Zhang, Y.; Li, T.; Ma, Z.; Jia, H.; Chen, Q.; Zhao, Y.; Zhai, L.; Zhong, R.; Li, C.; et al. Long non-coding RNA Linc-RAM enhances myogenic differentiation by interacting with MyoD. *Nat. Commun.* **2017**, *8*, 14016. [[CrossRef](#)] [[PubMed](#)]
115. Zhao, Y.; Cao, F.; Yu, X.; Chen, C.; Meng, J.; Zhong, R.; Zhang, Y.; Zhu, D. Linc-RAM is required for FGF2 function in regulating myogenic cell differentiation. *Rna Biol.* **2018**, *15*, 404–412. [[CrossRef](#)] [[PubMed](#)]
116. Sathish, V.; Thompson, M.A.; Bailey, J.P.; Pabelick, C.M.; Prakash, Y.S.; Sieck, G.C. Effect of proinflammatory cytokines on regulation of sarcoplasmic reticulum Ca<sup>2+</sup> reuptake in human airway smooth muscle. *Am. J. Physiol. Cell. Mol. Physiol.* **2009**, *297*, L26–L34. [[CrossRef](#)] [[PubMed](#)]
117. Zhang, Y.; Jiao, L.; Sun, L.-H.; Li, Y.; Gao, Y.; Xu, C.; Shao, Y.; Li, M.; Li, C.; Lu, Y.; et al. LncRNA ZFAS1 as a SERCA2a Inhibitor to Cause Intracellular Ca<sup>2+</sup> Overload and Contractile Dysfunction in a Mouse Model of Myocardial Infarction. *Circ. Res.* **2018**, *122*, 1354–1368. [[CrossRef](#)]
118. Soller, K.J.; Verardi, R.; Jing, M.; Abrol, N.; Yang, J.; Walsh, N.; Vostrikov, V.V.; Robia, S.L.; Bowser, M.T.; Veglia, G. Rheostatic Regulation of the SERCA/Phospholamban Membrane Protein Complex Using Non-Coding RNA and Single-Stranded DNA oligonucleotides. *Sci. Rep.* **2015**, *5*, 13000. [[CrossRef](#)]
119. Soller, K.J.; Yang, J.; Veglia, G.; Bowser, M.T. Reversal of Phospholamban Inhibition of the Sarco(endo)plasmic Reticulum Ca<sup>2+</sup>-ATPase (SERCA) Using Short, Protein-interacting RNAs and Oligonucleotide Analogs. *J. Biol. Chem.* **2016**, *291*, 21510–21518. [[CrossRef](#)]



120. Van Heesch, S.; Witte, F.; Schneider-Lunitz, V.; Schulz, J.F.; Adami, E.; Faber, A.B.; Kirchner, M.; Maatz, H.; Blachut, S.; Sandmann, C.-L.; et al. The Translational Landscape of the Human Heart. *Cell* **2019**, *178*, 242–260.e29. [[CrossRef](#)]
121. Ackermann, M.A.; Ziman, A.P.; Strong, J.; Zhang, Y.; Hartford, A.K.; Ward, C.W.; Randall, W.R.; Kontogianni-Konstantopoulos, A.; Bloch, R.J. Integrity of the network sarcoplasmic reticulum in skeletal muscle requires small ankyrin 1. *J. Cell Sci.* **2011**, *124*, 3619–3630. [[CrossRef](#)]
122. Solarewicz, J.; Manly, A.; Kokoszka, S.; Sleiman, N.; Leff, T.; Cala, S.E. Adiponectin secretion from cardiomyocytes produces canonical multimers and partial co-localization with calsequestrin in junctional SR. *Mol. Cell. Biochem.* **2019**, *457*, 201–214. [[CrossRef](#)]
123. He, W.; Huang, D.; Guo, S.; Wang, D.; Guo, J.; Cala, S.E.; Chen, Z. Association with SERCA2a directs phospholamban trafficking to sarcoplasmic reticulum from a nuclear envelope pool. *J. Mol. Cell. Cardiol.* **2020**, *143*, 107–119. [[CrossRef](#)] [[PubMed](#)]
124. Butler, J.; Watson, H.R.; Lee, A.G.; Schuppe, H.-J.; East, J.M. Retrieval from the ER-golgi intermediate compartment is key to the targeting of c-terminally anchored ER-resident proteins. *J. Cell. Biochem.* **2011**, *112*, 3543–3548. [[CrossRef](#)] [[PubMed](#)]
125. Teng, A.C.T.; Miyake, T.; Yokoe, S.; Zhang, L.; Rezende, J.L.M.; Sharma, P.; MacLennan, D.H.; Liu, P.P.; Gramolini, A.O. Metformin increases degradation of phospholamban via autophagy in cardiomyocytes. *Proc. Natl. Acad. Sci. USA* **2015**, *112*, 7165–7170. [[CrossRef](#)] [[PubMed](#)]
126. Nakagawa, T.; Yokoe, S.; Asahi, M. Phospholamban degradation is induced by phosphorylation-mediated ubiquitination and inhibited by interaction with cardiac type Sarco(endo)plasmic reticulum Ca<sup>2+</sup>-ATPase. *Biochem. Biophys. Res. Commun.* **2016**, *472*, 523–530. [[CrossRef](#)] [[PubMed](#)]
127. Niemeyer, J.; Mentrup, T.; Heidasch, R.; Müller, S.A.; Biswas, U.; Meyer, R.; Papadopoulou, A.A.; Dederer, V.; Haug-Kröper, M.; Adamski, V.; et al. The intramembrane protease SPPL 2c promotes male germ cell development by cleaving phospholamban. *Embo Rep.* **2019**, *20*. [[CrossRef](#)] [[PubMed](#)]
128. Willis, I.M.; Moir, R.D. Signaling to and from the RNA Polymerase III Transcription and Processing Machinery. *Annu. Rev. Biochem.* **2018**, *87*, 75–100. [[CrossRef](#)] [[PubMed](#)]
129. Subbaiah, K.C.V.; Hedaya, O.; Wu, J.; Jiang, F.; Yao, P. Mammalian RNA switches: Molecular rheostats in gene regulation, disease, and medicine. *Comput. Struct. Biotechnol. J.* **2019**, *17*, 1326–1338. [[CrossRef](#)]
130. O'Brien, J.; Hayder, H.; Zayed, Y.; Peng, C. Overview of MicroRNA Biogenesis, Mechanisms of Actions, and Circulation. *Front. Endocrinol.* **2018**, *9*, 402. [[CrossRef](#)]
131. Cai, B.; Zhang, Y.; Zhao, Y.; Wang, J.; Li, T.; Zhang, Y.; Jiang, Y.; Jin, X.; Xue, G.; Li, P.; et al. Long Noncoding RNA-DACH1 (Dachshund Homolog 1) Regulates Cardiac Function by Inhibiting SERCA2a (Sarcoplasmic Reticulum Calcium ATPase 2a). *Hypertension* **2019**, *74*, 833–842. [[CrossRef](#)]
132. Lentz, L.R.; Valberg, S.J.; Balog, E.M.; Mickelson, J.R.; Gallant, E.M. Abnormal regulation of muscle contraction in horses with recurrent exertional rhabdomyolysis. *Am. J. Vet. Res.* **1999**, *60*, 992–999.
133. Voit, A.; Patel, V.; Pachon, R.; Shah, V.; Bakhutma, M.; Kohlbrenner, E.; McArdle, J.J.; Dell'Italia, L.J.; Mendell, J.R.; Xie, L.-H.; et al. Reducing sarcolipin expression mitigates Duchenne muscular dystrophy and associated cardiomyopathy in mice. *Nat. Commun.* **2017**, *8*, 1–14. [[CrossRef](#)] [[PubMed](#)]
134. Fajardo, V.A.; Chambers, P.J.; Juracic, E.S.; Rietze, B.A.; Gamu, D.; Bellissimo, C.; Kwon, F.; Quadrilatero, J.; Tupling, A.R. Sarcolipin deletion in mdx mice impairs calcineurin signalling and worsens dystrophic pathology. *Hum. Mol. Genet.* **2018**, *27*, 4094–4102. [[CrossRef](#)] [[PubMed](#)]
135. Niranjan, N.; Mareedu, S.; Tian, Y.; Kodippili, K.; Fefelova, N.; Voit, A.; Xie, L.-H.; Duan, N.; Babu, G.J. Sarcolipin overexpression impairs myogenic differentiation in Duchenne muscular dystrophy. *Am. J. Physiol. Physiol.* **2019**, *317*, C813–C824. [[CrossRef](#)] [[PubMed](#)]

**Publisher's Note:** MDPI stays neutral with regard to jurisdictional claims in published maps and institutional affiliations.



© 2020 by the authors. Licensee MDPI, Basel, Switzerland. This article is an open access article distributed under the terms and conditions of the Creative Commons Attribution (CC BY) license (<http://creativecommons.org/licenses/by/4.0/>).